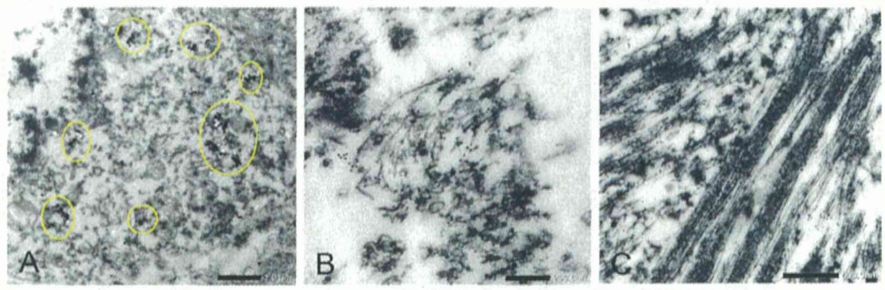

Figure 3 Immunoelectron microscopy of TPD brain with AT8 and immunogold labeling. A: in the Acb, the immunogold labeling in neurons was mostly localized to the granular structures (indicated by circles). Paired-helical filaments (PHF) were rare. Scale bar = 1.0 μm. **B**: sparse bundles of PHF were scattered in the neuronal cytoplasm. Scale bar = 200 nm. **C**: in the hippocampal CA1 region, prominent bundles of AT8 positive PHF were seen. Scale bar = 500 nm.

but not all, AD patients and non-demented, aged subjects (Additional file 2: Figure S1A). In these groups, however, only a limited number of cases showed tau pathology which was similarly abundant to that in TPD (Figure 4). In AD patients with heavy tau accumulation in the Acb, the caudate nucleus was also affected, a feature which distinguished AD from TPD. In TPD, the caudate tau lesions were either absent or, if present, very mild in all cases. In addition, senile plaques with tau positive dystrophic neurites were scattered in the Acb of such AD cases (Additional file 2: Figure S1B). In AD cases with mild tau pathology in the Acb, large neurons preferentially contained tau, a finding which was similar to the caudate nucleus in AD. In AD cases with heavy tau pathology in the Acb, such large neuron predominance became unclear and many tau positive, medium-sized neurons were seen. In both AD and non-demented, aged subjects, neuropil threads were also present in those with tau positive neurons in the Acb (Additional file 2: Figure S1C). The form of tau accumulation in AD patients and non-demented, aged subjects was similar to that in TPD, being predominantly pre-tangle like, diffuse accumulation in the cytoplasm.

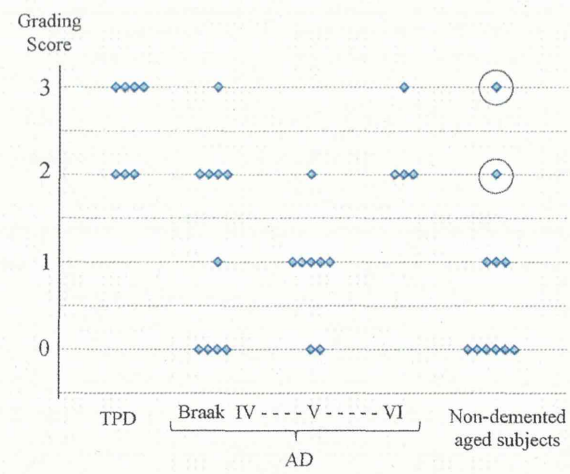

Figure 4 A graph of the density of neuronal tau accumulation in the Acb. The density of tau accumulation was graded as being 0 for absent, 1 for low, 2 for intermediate and 3 for high. Statistically significant differences were seen between TPD cases and non-demented, aged subjects ($P = 0.0031$) as well as AD cases in NFT stage IV ($P = 0.0192$) and V ($P = 0.0022$). The points encircled by a broken line in the non-demented, aged group indicate that the cases were over age 90.

The density of neuronal tau accumulation was graded to be 0 (absent) through 3(high) in AT8 immunostained tissue sections. Figure 4 illustrates the results in the Acb. Tau density in the Acb in the AD group was highly variable, except that the cases in Braak and Braak's NFT stage VI were either grade 2 or 3. Statistically significant differences were seen between the TPD cases and the non-demented, aged subjects ($P = 0.0031$) as well as the AD cases with NFT stage IV ($P = 0.0192$) and those with NFT stage V ($P = 0.0022$). Two non-demented, aged subjects with tau accumulation in the Acb were both over age 90. These 2 cases, similarly to TPD, lacked tau accumulation in the caudate nucleus and showed more NFT in the subiculum than in the entorhinal cortex. The results of semiquantitative analyses confirmed our observation that tau accumulation in the Acb was a remarkable finding in TPD. We performed similar analyses for a number of brain regions. The results are summarized in Table 3 as the averages of the graded scores for tau accumulation in each group. The concentration of tau pathology in the limbic structures, including the Acb and septal nuclei, in TPD contrasted with the broad distribution over the neocortex in AD.

Immunoblot analyses

The results of immunoblot analyses of samples from TPD and AD patients are shown in Figure 5. The tau band patterns in the sarkosyl insoluble fraction appeared to be essentially the same between TPD and AD, while the amount of insoluble tau was far smaller in the Acb than in the parahippocampal cortex in AD. It has to be noted that, because of the very high concentrations of insoluble tau in the parahippocampal cortex samples, the amounts of samples

Table 3 Summary of the semiquantitative grading of tau accumulation

	Braak stage	No. of cases	Acb	Caudate nucleus	Septal nucleus	CA1	Ent	Temp
TPD	III-IV	7	2.6	0.7	2.2	3	2.57	0.4
Non-demented	I-II	3	0	0	0	0.67	1	0
	III	8	1.13	0.25	0.63	1.38	2	1
AD	IV	10	1.2	0.6	1.4	2.67	3	1.4
	V	8	0.9	0.9	1.3	2.89	2.9	2.5
	VI	4	1.3	1.3	1.7	3	3	3

The numbers indicate averages of the scores in each group. The degree of tau pathology was qualitatively scored as 0: absent 1: low 2: intermediate 3: high. *TPD*, Tangle predominant dementia; *AD*, Alzheimer's disease; *NFT*, Neurofibrillary tangles; *Acb*, nucl. Accumbens; *CA1*, Hippocampal CA1 region; *Ent*, Entorhinal cortex; *Tmep*, Temporal neocortex.

applied to the gels had to be reduced in AD cases. This resulted in the relatively weak signals for the Acb samples in AD cases. The dephosphorylated samples of the Acb and parahippocampal cortex showed the 3R + 4R isoform pattern in both TPD and AD.

The Acb tau pathology and the presence/absence of clinical history of delusion

Finally, we examined if the degree of the Acb tau pathology was different between the subjects groups with and without the history of delusion in the clinical records (Additional file 3: Figure S2). In the group of subjects with Braaks' NFT stages III and IV, which included NFT stage III non-demented aged subjects, all TPD cases and NFT stage IV AD cases, the Acb tau score was higher in those with clinical history of delusion than those without it ($p = 0.033$). Similarly, the less conspicuous but still significant difference was seen in the group of all NFT stage AD cases ($p = 0.049$).

Discussions

There is significant overlap in the distribution of NFT between TPD and AD. However, an early genetic study of TPD cases indicated a paucity of the apolipoprotein E ε4 allele, which currently is the most powerful risk factor for AD [30]. More recently, a report has been made on the significant associations of TPD with the *MAPT* H1 haplotype as well as with some polymorphisms within the region of *MAPT* encoding the 3′ UTR [31]. Thus, together with the striking paucity of Aβ deposition, it seems that TPD is a unique neuropathological entity that has to be studied separately from AD.

The clinical and neuropathological features of the TPD patients we used in the present study generally agreed with those described in preceding articles [3,32]. In

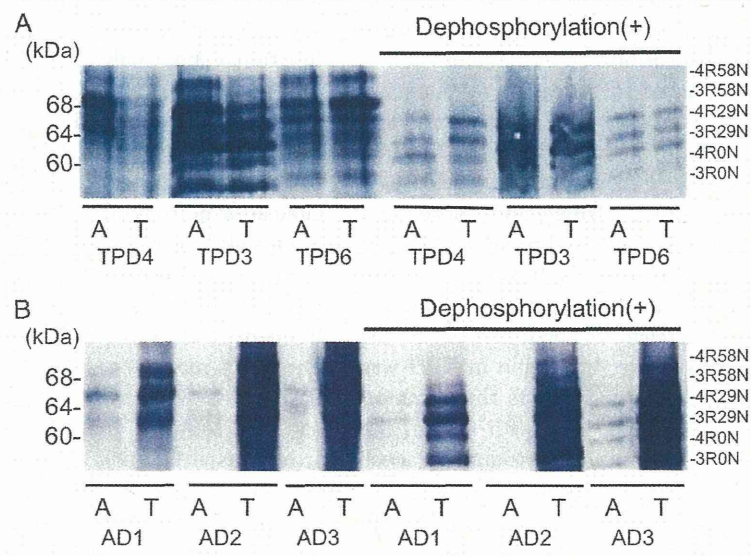

Figure 5 Immunoblot analyses of the sarkosyl insoluble tau. The sarkosyl insoluble fractions of the Acb (A) and the parahippocampal cortex (T) from TPD **(A)** and AD **(B)** were analyzed by immunoblot. A pan-tau antibody, HT7, was used. The Acb samples show the 3R + 4R isoform pattern similar to that in the parahippocampal cortices in both TPD and AD.

addition to the already well-known distribution of tau pathology, we found a considerable number of tau positive neurons and neuropil threads in the Acb. The Acb consists of the predominant medium-sized neurons and the occasional large neurons. Both cell types were affected by tau pathology in TPD. This contrasted AD with mild Acb tau pathology, in which large neurons were affected preferentially. Such a result is consistent with the previous reports which described that large neurons are more vulnerable in AD [33] and prone to tau accumulation [34]. In AD cases with the heavy Acb tau pathology, many medium-sized neurons were also tau positive. In the absence of TPD cases with the mild Acb tau pathology, it remains to be determined whether the difference is attributable to the distinct pathomechanisms between AD and TPD or to the variable vulnerability of different neuronal cell types.

The Acb may not be a region which is routinely sampled in a number of laboratories. Further, tau pathology in the Acb is not well stained by the Gallyas-Braak method. These facts together might explain the absence of previous reports on the occurrence of tau lesions in the Acb. The mechanism by which the Gallyas-Braak staining labels NFT remains to be determined. In TPD, insoluble tau consists of a mixture of the 3R and 4R isoforms in both the Acb and hippocampus, but NFT are intensely labeled by Gallyas-Braak staining in the latter. It may be noteworthy that, in the Acb, tau pathology occurs in a form of diffuse or granular cytoplasmic accumulations in the majority of tau positive neurons and that, ultrastructurally, PHF were rare. These contrasted with the hippocampal lesions where dense bundles of PHF were frequently seen. Obviously, factors that affect the reactivity of abnormal tau deposits to Gallyas-Braak staining need further clarification.

Tau pathology is considered to propagate in the brain from an affected region to another along the fiber connections, by spreading through the neuropil, or by both. A proposed mechanism for such propagation is a prion-like, seed-dependent conformational change and subsequent aggregation of the molecule, with a breakdown of the aggregate that generates the next seeds. In such a manner, the tau isoform pattern in the initial aggregates may be maintained in the later aggregate formations [35]. In the present study, we found that the Acb lesion in TPD was 3R + 4R tauopathy, a result which suggests the common origin of the tau pathology in the Acb with that in the hippocampus. The prevalence of diffuse cytoplasmic accumulations suggests that tau pathology in the Acb occurs later in the disease progression. In the hippocampus in TPD, many ghost tangles are seen, suggesting that the hippocampal lesions precede the Acb lesions.

Occurrence of NFT in the Acb in AD was reported previously [36,37]. In the present study, however, we have found that tau accumulation in TPD is more frequent and consistent than AD. The Acb receives direct and massive projections from the hippocampal CA1 and subiculum [14,38,39]. It has been repeatedly reported in TPD that the density of NFT is higher in the hippocampal CA1 and subiculum than in the entorhinal cortex [1,2,7,28]. Thus, the heavy tau pathology in the subiculum and CA1, through neural circuit-mediated propagation to the Acb, may result in the more pronounced tau accumulation in the Acb in TPD than in AD. Such an idea may be consistent with our finding that the difference in Acb tau pathology was statistically significant between TPD and AD in NFT stages IV and V but not in AD at stage VI. In AD with Acb lesions, tau accumulation was also found more frequently in the caudate nucleus than was the case in TPD. The caudate nucleus receives massive innervations from the cerebral cortex where, unlike TPD, tau pathology is severe in AD. On the other hand, the septal nuclei, like the Acb, receive direct projections from the subiculum and CA1 [14,38]. Again, we found, in the present study, heavier tau accumulation in these areas in TPD than in AD at NFT stages IV and V.

TPD is primarily an amnestic disease with relatively mild non-amnestic symptoms of dementia. In 6 of 7 TPD cases used in this study, however, delusion was a consistent clinical feature. This may be partly attributable to the fact that our brain tissue archive is principally based on the psychiatric hospital autopsies. However, occurrence of psychiatric symptoms has also been described in a number of previous reports on TPD. As an example, Jellinger et al. reported depression in 17.5% and paranoid ideas in 15% of TPD cases [3]. The Acb is part of the mesolimbic system in which the Acb receives dopaminergic input from the VTA. Recent evidence suggests that, in schizophrenia, functional abnormality in the Acb causes excessive release of dopamine from the VTA, which then results in the psychiatric symptoms [19,40-43]. While neuronal loss was not apparent in the Acb in TPD, it may be noteworthy that association of intraneuronal tau aggregation with clinical symptoms has been suggested in early stage AD lesions [44]. In AD, cases with more neocortical NFT were reported to be associated with more psychosis [45]. Thus, tau accumulation in the Acb could be related to the frequent delusion in TPD. Delusion and other psychotic symptoms may occur by multiple mechanisms in dementia patients. We have to note that 2 of the 7 TPD cases had argyrophilic grain pathology and that psychotic symptoms are known to be common in the patients with argyrophilic grain disease [46]. Whether the Acb tau accumulation is related to the psychiatric symptoms in TPD may be an issue for further investigation.

In the present study, we found that tau pathology occurred unevenly in the Acb in TPD (Figures 1 and 2E). The striatum is not uniform and has distinct neurochemical

compositions and connections that are referred to as matrix and striosomes. The similar but more complex compartmentation was reported in the human Acb [47]. We have performed additional immunohistochemistry for tyrosine hydroxylase (TH) and tau in serially-cut, free-floating sections in two TPD cases, in which the remnants of Acb blocks were available after the initial sectioning for the main body of this study. Comparison of the adjacent sections stained for TH and tau indicates that tau pathology preferentially occurs in areas where the fine, mesh-like TH staining is relatively light (Additional file 4: Figure S3). Such a result suggests the relationship between the uneven distribution of tau pathology and neurochemical heterogeneity in the Acb. However, because of the limited number of currently available samples and of the more complex neurochemical architecture in the Acb than the simple matrix-striosome structure in the caudate nucleus [47], future, extensive studies should be needed for further exploration.

Conclusions

We have found frequent tau accumulation in the Acb in patients with TPD. Both the medium-sized and large neurons are affected. While similar tau accumulation was seen in a small number of all AD patients, it was far more frequent and consistent in TPD than AD. The tau isoforms abnormally accumulated in the Acb were 3R and 4R, which suggests a common origin with the hippocampal tau pathology. The Acb receives direct and massive projections from the hippocampal CA1 and subiculum where tau pathology is extremely severe in TPD. Such a result may support the idea that abnormal tau aggregation propagates via neural circuits. Tau accumulation in TPD should be a subject of further investigations to approach the long-lasting issue of the simultaneous deposition of Aβ and tau in AD. In addition, the relationship between the tau pathology in the Acb and such psychiatric symptoms as delusion in TPD needs further exploration.

Additional files

Additional file 1: Table S1. The primary antibodies used in this study.

Additional file 2: Figure S1. Tau accumulation in the Acb in AD and non-demented, aged subjects. Immunohistochemistry with AT8. A: absence of tau positive neurons in an AD case in Braak and Braak's NFT stage IV. Scale bar = 100 μm in A-C. B: a diffuse cytoplasmic staining, neuropil threads and duystrophic neurite in a senile plaque in an AD case in NFT stage VI. C: a tau positive neuron and neuropil threads in a non-demented, aged subject.

Additional file 3: Figure S2. A graph of the density of neuronal tau accumulation in the Acb. The left plots: the group of Braaks' NFT stages III and IV, which includes non-demented aged subjects, TPD cases and AD cases with Braaks' NFT stage IV. Cases with delusion in the clinical history show higher tau score than those without delusion in the Acb. The right plots: the group of AD cases with Braaks' NFT stages IV through VI. Again, cases with delusion show higher tau score than those without delusion.

Additional file 4: Figure S3. The serial section immunohistochemistry for tau and tyrosine hydroxylase (TH). Forty micrometer thick, free floating sections were cut serially from two tangle predominant dementia (TPD) cases, in which the remnants of Acb blocks were available after the initial sectioning for the main body of the study. A set of every other section was stained for TH and the other set for tau with AT8. A and C: AT8 staining in a TPD case 1. B: TH staining of the section between A and C. In B, two types of areas are distinguished based on the modest difference in the density of fine, mesh-like TH staining. There is a propensity that tau pathology preferentially occurs in areas where the fine, mesh-like TH staining is relatively light (A, C). Scale bar = 2 mm in A (A, B and C are at the same magnification). D: higher power photomicrographs of the boxed areas in B and C. The left half is the staining with AT8 and the right half staining for TH. Scale bar = 400 micro-m (D).

Abbreviations

(TPD): Tangle-predominant dementia; (NFT): Neurofibrillary tangles; (AD): Alzheimer's disease; (3R): 3-repeat; (4R): 4-repeat; (Acb): Nucleus accumbens; (VTA): Ventral tegmental area; (HE): Hematoxylin and eosin; (PFA): Paraformaldehyde; (PHF): Paired helical filaments; (Aβ): Amyloid β protein; (TH): tyrosine hydroxylase.

Competing interests

The authors declare that they have no competing interests.

Authors' contributions

IK carried out the microscopic observation, immunoblot and statistical analyses. IK also drafted the initial manuscript. MHa conducted the sample preparation and immunoblot and carried them out with IK. TA participated in the design and coordination of the study. KI carried out the microscopic observation with IK. KO, KN and NA organized the brain archives including clinical information, selected appropriate cases, and performed neuropathological analyses of all cases used in this study. OK participated in the design of the study and performed statistical analyses with IK. SH conceived of the study and participated in the initial design. MHo contributed to the reagents, materials and analysis tools, and conducted free-floating immunohistochemistry. YH participated in the design of the study and helped to draft the manuscript. HA supervised the design and coordination of the study and worked up the manuscript. All authors read and approved the final manuscript.

Authors' information

IK is a graduate student of Department of Psychiatry, Graduate school of Medicine, Yokohama City University School of Medicine. MHa is the senior director of Department of Neuropathology and Cell Biology, Tokyo Metropolitan Institute of Medical Science (TMIMS). TA, KI, NA and SH contributed to this study as visiting scientists of Dementia project, TMIMS. TA is also an associated professor of Department of Psychiatry, Graduate School of Comprehensive Human Sciences, University of Tsukuba. KO and KN are psychiatrists and neuropathologists in Tokyo Metropolitan Matsuzawa Hospital (TMMH), visiting scientists of Dementia project, TMIMS and in charge of the brain archive of TMMH/TMIMS. OK is an associate professor of Department of Psychiatry, Graduate school of Medicine, Yokohama City University School of Medicine. MHo is a chief researcher of Dementia project, TMIMS. YH is a professor of Department of Psychiatry, Graduate school of Medicine, Yokohama City University School of Medicine. HA is the senior director of Dementia project, TMIMS.

Acknowledgements

We are grateful to the patients and their families who made this research possible. We thank Dr. Peter Davies (Albert Einstein College of Medicine) for providing us with his excellent anti-tau antibodies, PHF-1 and MC-1. We also thank Ms. Yoko Shimomura and Mr. Kentaro Endo (Tokyo Metropolitan Institute of Medical Science) for their technical assistance with immuno-electron microscopy, and Ms. Yoko Shimomura, Ms. Hiromi Kondo and Ms. Chie Haga (Tokyo Metropolitan Institute of Medical Science) for their assistance in tissue preparation and staining. Helpful advice by Dr. Takashi Nonaka (Tokyo Metropolitan Institute of Medical Science), as well as Dr. Takashi Togo and Dr. Masatake Uchikado (Department of Psychiatry, Yokohama City University School of Medicine), is very much appreciated. None of the

authors has any conflict of interest. This research was supported by Grants-in-Aid from the Ministry of Health, Labor and Welfare (12946221, MH, MH and HA) and Ministry of Education, Culture, Science (24500429, HA), Japan.

Author details
[1]Dementia Research Project, Tokyo Metropolitan Institute of Medical Science, 2-1-6 Kamikitazawa, Setagaya-ku, Tokyo 156-8506, Japan. [2]Department of Psychiatry, Graduate school of Medicine, Yokohama City University School of Medicine, Yokohama, Japan. [3]Department of Neuropathology and Cell Biology, Tokyo Metropolitan Institute of Medical Science, Tokyo, Japan. [4]Department of Psychiatry, Graduate School of Comprehensive Human Sciences, University of Tsukuba, Tsukuba, Japan. [5]Department of inflammation of Pathology, Faculty of Medicine, Kagawa University, Takamatsu, Japan. [6]Tokyo Metropolitan Matsuzawa Hospital, Tokyo, Japan.

Received: 16 February 2014 Accepted: 1 April 2014
Published: 8 April 2014

References

1. Ikeda K, Akiyama H, Arai T, Oda T, Kato M, Iseki E, Kosaka K, Wakabayashi K, Takahashi H (1999) Clinical aspects of 'senile dementia of the tangle type'- a subset of dementia in the senium separable from late onset. Alzheimer's disease. Dement Geriatr Cogn Disord 10:6–11
2. Noda K, Sasaki K, Fujimi K, Wakisaka Y, Tanizaki Y, Wakug- awa Y, Kiyohara Y, Iida M, Aizawa H, Iwaki T (2006) Quantitative analysis of neurofibrillary pathology in a general population to reappraise neuropathological criteria for senile dementia of the neurofibrillary tangle type (tangle-only dementia) the Hisayama Study. Neuropathology 26:508–518
3. Jellinger KA, Attems J (2007) Neurofibrillary tangle-predominant dementia: comparison with classical Alzheimer disease. Acta Neuropathol 113:107–117
4. McKhann GM, Albert MS, Grossman M, Miller B, Dickson D, Trojanowski JQ, Work Group on Frontotemporal Dementia and Pick's Disease (2001) Clinical and pathological diagnosis of frontotemporal dementia: report of the work group on frontotemporal dementia and Pick's disease. Arch Neurol 58:1803–1809
5. Cairns NJ, Bigio EH, Mackenzie IR, Neumann M, Lee VM, Hatanpaa KJ, White CL 3rd, Schneider JA, Grinberg LT, Halliday G, Duyckaerts C, Lowe JS, Holm IE, Tolnay M, Okamoto K, Yokoo H, Murayama S, Woulfe J, Munoz DG, Dickson DW, Ince PG, Trojanowski JQ, Mann DM (2007) Neuropathologic diagnostic and nosologic criteria for frontotemporal lobar degeneration: consensus of the Consortium for Frontotemporal Lobar Degeneration. Acta Neuropathol 114:5–22
6. Braak H, Braak E (1991) Neuropathological staging of Alzheimer-related changes. Acta Neuropathol 82:239–259
7. Yamada M (2003) Senile dementia of the neurofibrillary tangle type (tangle-only dementia): neuropathological criteria and clinical guidelines for diagnosis. Neuropathology 23:311–317
8. Kovacs GG, Molnár K, László L, Ströbel T, Botond G, Hönigschnabl S, Reiner-Concin A, Palkovits M, Fischer P, Budka H (2011) A peculiar constellation of tau pathology defines a subset of dementia in the elderly. Acta Neuropathol 122:205–222
9. Groenewegen HJ, Vermeulen-Van der Zee E, te Kortschot A, Witter MP (1987) Organization of the projections from the subiculum to the ventral striatum in the rat. A study using anterograde transport of Phaseolus vulgaris leucoagglutinin. Neuroscience 23:103–210
10. Kita H, Kitai ST (1990) Amygdaloid projections to the frontal cortex and the striatum in the rat. J Comp Neurol 298:40–49
11. Berendse HW, Galis-de Graaf Y, Groenewegen HJ (1992) Topographical organization and relationship with ventral striatal compartments of prefrontal corticostriatal projections in the rat. J Comp Neurol 316:314–347
12. French SJ, Totterdell S (2002) Hippocampal and prefrontal cortical inputs monosynaptically converge with individual projection neurons of the nucleus accumbens. J Comp Neurol 446:151–165
13. Heimer L, Zahm DS, Churchill L, Kalivas PW, Wohltmann C (1991) Specificity in the projection patterns of accumbal core and shell in the rat. Neuroscience 41:89–125
14. Groenewegen HJ, Berendse HW, Meredith GE, Haber SN, Voorn P, Wolters JG, Lohman AHM (1991) Functional anatomy of the ventral limbic system-innervated striatum. In: Willner P, Scheel-Kruger J (eds) The mesolimbic dopamine system: from motivation to action. Wiley, Chichester, pp 19–59
15. Rahman S, McBride WJ (2001) D1-D2 dopamine receptor interaction within the nucleus accumbens mediates long-loop negative feedback to the ventral tegmental area (VTA). J Neurochem 77:1248–1255
16. Kalivas PW, Nakamura M (1999) Neural systems for behavioral activation and reward. Curr Opin Neurobiol 9:223–227
17. Cardinal RN, Parkinson JA, Hall J, Everitt BJ (2002) Emotion and motivation: the role of the amygdala, ventral striatum, and prefrontal cortex. Neurosci Biobehav Rev 26:321–352
18. Grace AA, Bunney BS, Moore H, Todd CL (1997) Dopamine-cell depolarization block as a model for the therapeutic actions of antipsychotic drugs. Trends Neurosci 20:31–37
19. Grace AA (2000) Gating of information flow within the limbic system and the pathophysiology of schizophrenia. Brain Res Brain Res Rev 31:330–341
20. Jellinger KA, Bancher C (1998) Senile dementia with tangles (tangle predominant form of senile dementia). Brain Pathol 8:367–376
21. Mirra SS, Heyman A, McKeel D, Sumi SM, Crain BJ, Brownlee LM, Vogel FS, Hughes JP, van Belle G, Berg L (1991) The Consortium to Establish a Registry for Alzheimer's Disease (CERAD). Part II. Standardization of the neuropathologic assessment of Alzheimer's disease. Neurology 41:479–486
22. McKeith IG, Dickson DW, Lowe J, Emre M, O'Brien JT, Feldman H, Cummings J, Duda JE, Lippa C, Perry EK, Aarsland D, Arai H, Ballard CG, Boeve B, Burn DJ, Costa D, Del Ser T, Dubois B, Galasko D, Gauthier S, Goetz CG, Gomez-Tortosa E, Halliday G, Hansen LA, Hardy J, Iwatsubo T, Kalaria RN, Kaufer D, Kenny RA, Korczyn A, et al (2005) Diagnosis and management of dementia with Lewy bodies. Third report of the DLB consortium. Neurology 65:1863–18725
23. Aoki N, Higashi S, Kawakami I, Kobayashi Z, Hosokawa M, Katsuse O, Togo T, Hirayasu Y, Akiyama H (2012) Localization of fused in sarcoma (FUS) protein to the post-synaptic density in the brain. Acta Neuropathol 124:383–394
24. Sun A, Nguyen XV, Bing G (2002) Comparative analysis of an improved thioflavin-s stain, Gallyas silver stain, and immunohistochemistry for neurofibrillary tangle demonstration on the same Sections. J Histochem Cytochem 50:463–472
25. Arai T, Ikeda K, Akiyama H, Nonaka T, Hasegawa M, Ishiguro K, Iritani S, Tsuchiya K, Iseki E, Yagishita S, Oda T, Mochizuki A (2004) Identification of amino-terminally cleaved tau fragments that distinguish progressive supranuclear palsy from corticobasal degeneration. Ann Neurol 55:72–79
26. Yamada M, Itoh Y, Sodeyama N, Suematsu N, Otomo E, Matsushita M, Mizusawa H (2001) Senile dementia of the neurofibrillary tangle type: a comparison with Alzheimer's disease. Dement Geriatr Cogn Disord 12:117–126
27. Bancher C, Jellinger KA (1994) Neurofibrillary tangle pre- dominant form of senile dementia of Alzheimer type: a rare subtype in very old subjects. Acta Neuropathol 88:565–570
28. Iseki E, Tsunoda S, Suzuki K, Takayama N, Akatsu H, Yamamoto T, Kosaka K (2002) Regional quantitative analysis of NFT in brains of non-demented elderly persons: comparisons with findings in brains of late-onset Alzheimer's disease and limbic NFT dementia. Neuropathology 22(1):34–39
29. Saito Y, Ruberu NN, Sawabe M, Arai T, Tanaka N, Kakuta Y, Yamanouchi H, Murayama S (2004) Staging of argyrophilic grains: an age-associated tauopathy. J Neuropathol Exp Neurol 63:911–918
30. Ikeda K, Akiyama H, Arai T, Sahara N, Mori H, Usami M, Sakata M, Mizutani T, Wakabayashi K, Takahashi H (1997) A subset of senile dementia with high incidence of the apolipoprotein E epsilon2 allele. Ann Neurol 41:693–695
31. Santa-Maria I, Haggiagi A, Liu X, Wasserscheid J, Nelson PT, Dewar K, Clark LN, Crary JF (2012) The MAPT H1 haplotype is associated with tangle-predominant dementia. Acta Neuropathol 124:693–704
32. Janocko NJ, Brodersen KA, Soto-Ortolaza AI, Ross OA, Liesinger AM, Duara R, Graff-Radford NR, Dickson DW, Murray ME (2012) Neuropathologically defined subtypes of Alzheimer's disease differ significantly from neurofibrillary tangle-predominant dementia. Acta Neuropathol 124:681–692
33. Oyanagi K, Takahashi H, Wakabayashi K, Ikuta F (1987) Selective involvement of large neurons in the neostriatum of Alzheimer's disease and senile dementia: a morphometric investigation. Brain Res 411:205–211
34. Oyanagi K, Takahashi H, Wakabayashi K, Ikuta F (1991) Large neurons in the neostriatum in Alzheimer's disease and progressive supranuclear palsy. Brain Res 544:221–226
35. Hasegawa M, Watanabe S, Kondo H, Akiyama H, Mann DM, Saito Y, Murayama (2014) 3R and 4R tau isoforms in paired helical filaments in Alzheimer's disease. Acta Neuropathol 127:303–305
36. Oyanagi K, Makifuchi T, Ohtoh T, Chen KM, Gajdusek DC, Chase TN, Ikuta F (1994) The neostriatum and nucleus accumbens in parkinsonism-dementia

complex of Guam: a pathological comparison with Alzheimer's disease and progressive supranuclear palsy. Acta Neuropathol 88:122–128
37. Selden N, Mesulam MM, Geula C (1994) Human striatum: the distribution of neurofibrillary tangles in Alzheimer's disease. Brain Res 648:327–331
38. Kim Y, Spruston N (2012) Target-specific output patterns are predicted by the distribution of regular-spiking and bursting pyramidal neurons in the subiculum. Hippocampus 22:693–706
39. Kelley AE, Domesick VB (1982) The distribution of the projection from the hippocampal formation to the nucleus accumbens in the rat: an anterograde- and retrograde-horseradish peroxidase study. Neuroscience 7:2321–2335
40. Weinberger DR, Lipska BK (1995) Cortical maldevelopment, anti-psychotic drugs, and schizophrenia: a search for common ground. Schizophr Res 16:87–110
41. O'Donnell P, Grace AA (1998) Dysfunctions in multiple interrelated systems as the neurobiological bases of schizophrenic symptom clusters. Schizophr Bull 24:267–283
42. Laruelle M (2000) The role of endogenous sensitization in the pathophysiology of schizophrenia: implications from recent brain imaging studies. Brain Res Brain Res Rev 31:371–384
43. Lewis DA, Levitt P (2002) Schizophrenia as a disorder of neurodevelopment. Annu Rev Neurosci 25:409–432
44. Braak H, Zetterberg H, del Tredici K, Blennow K (2013) Intraneuronal tau aggregation precedes diffuse plaque deposition, but amyloid-β changes occur before increases of tau in cerebrospinal fluid. Acta Neuropathol 126:631–641
45. Farber NB, Rubin EH, Newcomer JW, Kinscherf DA, Miller JP, Morris JC, Olney JW, McKeel DW Jr (2000) Increased neocortical neurofibrillary tangle density in subjects with Alzheimer disease and psychosis. Arch Gen Psychiatry 57:1165–1173
46. Togo T, Isojima D, Akatsu H, Suzuki K, Uchikado H, Katsuse O, Iseki E, Kosaka K, Hirayasu Y (2005) Clinical features of argyrophilic grain disease: a retrospective survey of cases with neuropsychiatric symptoms. Am J Geriatr Psychiatry 13:1083–1091
47. Holt DJ, Graybiel AM, Saper CB (1997) Neurochemical architecture of the human striatum. J Comp Neurol 384:1–25

doi:10.1186/2051-5960-2-40
Cite this article as: Kawakami *et al.*: Tau accumulation in the nucleus accumbens in tangle-predominant dementia. *Acta Neuropathologica Communications* 2014 **2**:40.

Carbonyl stress in schizophrenia

Masanari Itokawa*[1], Mitsuhiro Miyashita*, Makoto Arai* and Toshio Miyata†

*Project for Schizophrenia and Affective Disorders Research, Tokyo Metropolitan Institute of Medical Science, Tokyo 156-8506, Japan

†United Centers for Advanced Research and Translational Medicine (ART), Tohoku University Graduate School of Medicine, Miyagi 980-8575, Japan

Abstract

We have identified idiopathic carbonyl stress in a subpopulation of schizophrenic patients. We first identified a patient with a mutation in *GLO1* (glyoxalase I) who showed increased AGE (advanced glycation end-product) levels and decreased vitamin B_6 levels. By applying the observations from this rare case to the general schizophrenic population, we were able to identify a subset of patients (20%) for whom carbonyl stress may represent a causative pathophysiological process. Genetic defects in *GLO1* increase the risk of carbonyl stress 5-fold, and the resulting increased AGE levels correlate significantly with PANSS (Positive and Negative Syndrome Scale) scored negative symptoms. Pyridoxamine, an active form of vitamin B_6 and scavenger for carbonyl stress, could represent a novel and efficacious therapeutic agent for these treatment-resistant symptoms. In the present article, we describe a unique research approach to identify the causative process in the pathophysiology of a subset of schizophrenia. Our findings could form the basis of a schizophrenia subtype classification within this very heterogeneous disease and ultimately lead to better targeted therapy.

Introduction

Schizophrenia is a debilitating and complex mental disorder with a worldwide prevalence of approximately 1%. Despite extensive research, the full pathophysiology of this disease remains unclear [1,2]. Current therapies focus on treating symptoms using anti-psychotic agents which are unfortunately highly prone to inducing significant side effects. This has led to intensive research into the identification of new disease mechanisms, with the aim of developing novel classes of therapeutic agents, which are both efficacious and free of debilitating adverse effects. There is a strong body of evidence from biochemical and pharmacological studies, using human samples and animal models, which suggests that oxidative or carbonyl stress contributes to the pathophysiology of schizophrenia [3–6]. Oxidative stress is a central mediator of AGE (advanced glycation end-product) formation, and pyridoxamine, an active form of vitamin B_6, detoxifies RCOs (reactive carbonyl compounds) via carbonyl-amine chemistry. The cellular removal of AGEs is largely dependent upon activity of the zinc metalloenzyme Glo1 (glyoxalase I) [7]. The glyoxalase detoxification system is ubiquitous in human tissues, including the brain. This cascade interacts with other metabolizing cascades, including putative gene products involved in the aetiology of schizophrenia, such as glutathione, homocysteine and folic acid metabolites [8–15].

Recent studies have revealed that Glo1 dysfunction is involved not only in systemic diseases such as diabetes mellitus [16] and vascular injury [17], but also in neuropsychiatric illnesses, such as mood disorders [18], autism [19,20], anxiety disorders [21] and alcoholism [22]. In mice, altered levels of *Glo1* expression are associated with anxiety-like behavioural phenotypes [23–25]. Interestingly, *GLO1* maps to chromosome 6p21, a linkage region for schizophrenia [26–28]. Lending further support to this association is the report of a missense Glu^{111}/Ala^{111} polymorphism, in two multiplex Caucasian pedigrees with schizophrenia spectrum disorders [29].

The present article focuses on idiopathic carbonyl stress in a subpopulation of schizophrenic patients with no history of diabetes mellitus or renal dysfunction. In the patients studied who showed high plasma AGE levels, a proportion of them also harboured a genetic defect in the *GLO1* gene, suggesting that, in these schizophrenics, carbonyl stress may be the result of dysfunctional Glo1 detoxification.

GLO1 mutation associated with a schizophrenia pedigree

In this section, we discuss an interesting report from our laboratory, of a schizophrenic with a deficiency in Glo1 [30]. The case was a 60-year-old male who suffered from severe schizophrenia. Within his family were two affected brothers, one of whom committed suicide and the other who was long-term hospitalized due to his illness. He also had two maternal uncles with schizophrenia. Both the case and his brother exhibited treatment-resistant disease, despite intensive therapy. DNA from the case showed a novel mutation, consisting of an adenine insertion at nucleotide 79 in exon 1, introducing a frameshift at codon 27 and a premature termination codon, after aberrant translation of 15 amino acid residues (T27NfsX15) [30]. In addition, expression of *GLO1* mRNA and protein was decreased by 50% in the lymphocytes of our patient (Figures 1a and 1b).

Key words: advanced glycation end-product (AGE), carbonyl stress, glyoxalase I, pyridoxamine, schizophrenia, vitamin B_6.

Abbreviations: AGE, advanced glycation end-product; Glo1, glyoxalase I; PANSS, Positive and Negative Syndrome Scale.

[1]To whom correspondence should be addressed (email itokawa-ms@igakuken.or.jp).

Figure 1 | *GLO1* and a frameshift mutation

(**a**) mRNA expression. (**b**) Results of Western blotting. (**c**) Enzymatic activity of Glo1. GAPDH, glyceraldehyde-3-phosphate dehydrogenase; RBC, red blood cell.

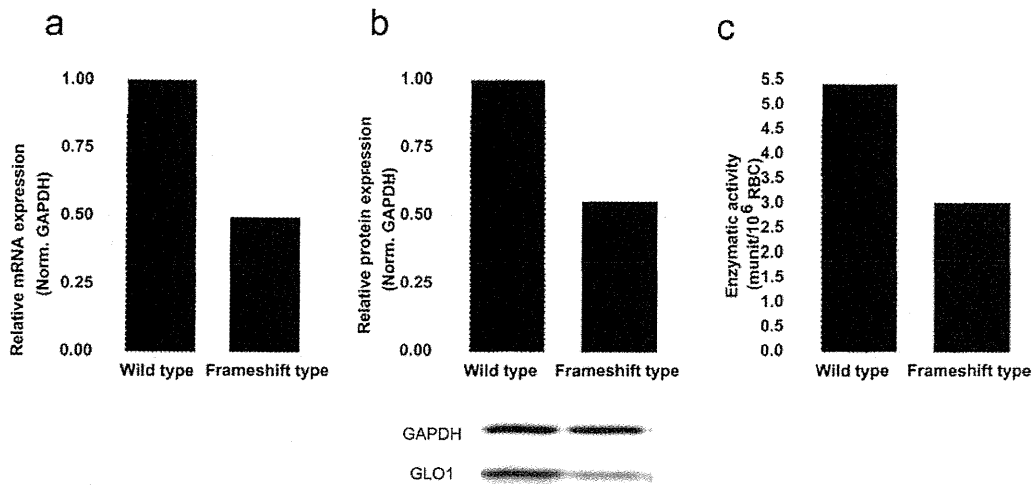

In the red blood cells of our case, enzymatic activity levels of Glo1 were approximately half that of wild-type controls (Figure 1c). We postulated that this loss-of-function mutation accompanied by AGE accumulation would be shared by affected individuals in this family, although we were unable to access the genetic material to test our theory.

Mutations of *GLO1* and increased levels of plasma AGEs in schizophrenics

In a new study, we resequenced the *GLO1* gene from 1761 schizophrenics and 1921 control subjects, and identified another novel frameshift mutation [30] Individuals carrying frameshift mutations also showed a 40–50% reduction in Glo1 activity from red blood cells, a result that supports the finding that genetic mutations in the *GLO1* gene typically occur in one allele. As we predicted, schizophrenic carriers of the *GLO1* frameshift mutations displayed significantly increased levels of plasma AGEs. Since these patients had no history of diabetes mellitus or renal failure, it is most likely that these increased levels of plasma AGEs are due to reduced Glo1 function. In addition, patients with elevated AGE levels showed a clear concomitant decrease in vitamin B_6 levels. In the two *GLO1* frameshift mutation carriers, we found markedly reduced vitamin B_6 levels. This is probably a reflection of increased vitamin B_6 consumption in the detoxification of α-oxoaldehydes, by-products of carbonyl stress. Additionally, in this study, we detected a single nucleotide polymorphism which resulted in an amino acid residue change from the wild-type Glu^{111} to alanine. Schizophrenics homozygous for the Ala^{111} variant displayed a 16% reduction in enzymatic activity, accompanied by a significant increase in plasma AGEs [30]. This reduced Glo1 enzymatic activity in Ala^{111} variants was determined by comparing GFP-fused Glo1 constructs carrying Ala^{111} and Glu^{111}, using *in vitro* assays. Interestingly, Glo1 variations were not confined to patients. We found non-psychiatric controls carrying frameshift mutations or homozygous Ala^{111} alleles, all of whom exhibited normal plasma AGEs and vitamin B_6 levels, in contrast with mutation carrying schizophrenics. This is all highly suggestive of active compensatory mechanisms in non-schizophrenics. In addition, plasma glutathione and zinc levels were significantly higher in non-psychiatric individuals carrying the mutation compared with schizophrenics with a frameshift mutation (glutathione, $P = 0.03$; zinc, $P = 0.002$). These results imply that, in non-psychotic subjects, additional environmental factors compensate for defects in Glo1 activity, possibly involving zinc and glutathione, as both are necessary for Glo1-mediated detoxification of carbonyl compounds.

In support of our hypothesis for idiopathic carbonyl stress being a causative state in schizophrenia, we expanded our study from a small population carrying genetic defects in *GLO1*, to 178 schizophrenia and 76 control subjects, with no evidence of diabetes mellitus or renal dysfunction, and measured plasma AGEs and vitamin B_6 levels. We found significantly higher concentrations of AGEs in patients compared with controls ($P<0.0001$), whereas vitamin B_6 levels were significantly lower in schizophrenics relative to control subjects ($P<0.0001$) (Figure 2). If we defined high circulating AGEs as plasma levels greater than the mean±2S.D. of controls, 66 of the patients (37.5%) and three of the controls (3.9%) showed high circulating plasma AGEs (distributions were significantly different between schizophrenia and control subjects: $\chi^2 = 30.05$, $P<0.00001$, odds ratio = 14.6, 95% confidential interval = 4.42–48.21). For vitamin B_6 levels, 39.9% of schizophrenics showed low levels of plasma vitamin B_6 compared with 7.4% of

Figure 2 | Plasma AGE and vitamin B_6 levels in schizophrenics and controls
(**a**) AGE levels. (**b**) Vitamin B_6 levels.

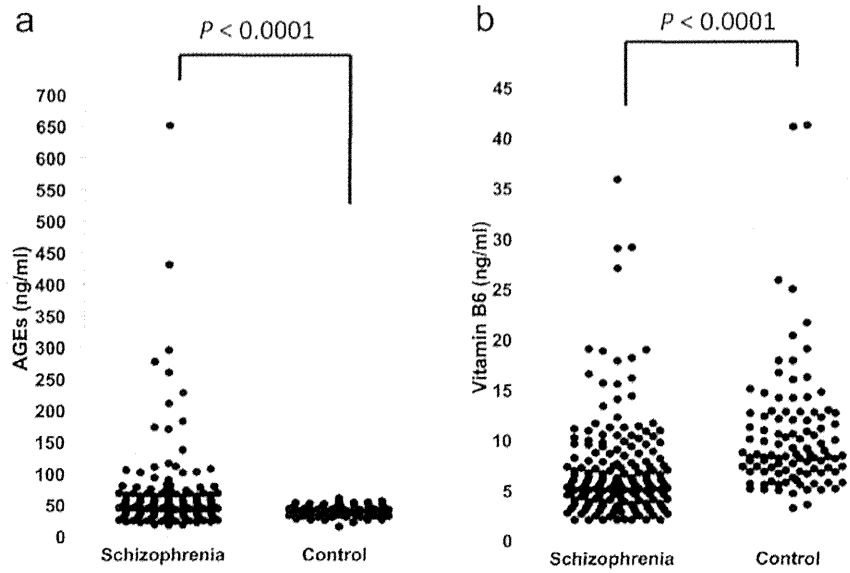

control subjects (χ^2 = 20.9, P<0.0001, odds ratio = 5.99, 95% confidential interval = 2.59–13.83). Low levels were described as being under 6 ng/ml in males and 4 ng/ml in females. As these patients had received anti-psychotic therapy previously, we could not rule out an effect of medication on the induction of carbonyl stress in this cohort. To address this issue, we recently examined a drug-naive patient with prodromal phase schizophrenia, who exhibited enhanced carbonyl stress with high plasma pentosidine levels [31]. Plasma pentosidine levels are typically used as a marker for carbonyl stress. Biochemical analysis demonstrated no abnormalities indicative of disease, such as diabetes mellitus or chronic kidney diseases. Crucially, this case suggests that the idiopathic carbonyl stress seen in schizophrenics may not be a result of anti-psychotic medication.

In order to examine the genetic contribution of *GLO1* to carbonyl stress in schizophrenia, we tested the correlation between genotypes and plasma AGE levels, by performing χ^2 tests (Table 1). The frameshift mutations and homozygous Ala^{111} variants are significantly associated with high carbonyl stress (χ^2 = 7.72, P = 0.005, odds ratio = 5.63, 95% confidential interval = 1.46–21.64).

Schizophrenia has long been considered a heterogeneous syndrome, with Kraepelin establishing the conceptual disease category as dementia precox, at the end of the 19th Century. Although current studies suggest that carbonyl stress is not applicable to the pathophysiology of all schizophrenia, approximately 37% of schizophrenics studied showed increased AGEs, suggesting a link between stress and subtypes of the disease. Twin and adoption studies led the way in defining schizophrenia as a disease with a large heritable component. On 23 December 2011, the SchizGene database listed 1727 studies identifying 8788 polymorphisms from 1008 genes thought to be associated with schizophrenia (http://www.szgene.org/). Yet, no causal gene with a large effect has been identified, despite this huge genetic research effort. Indeed, many studies conflict with each other. This lack of consensus is unsurprising considering the known heterogeneity of the disease. Recent genome-wide association studies have been expanding in sample size, in some cases to over 10000 case and control samples [32–36], yet only genetic variations with a small effect size have been identified. It is plausible that, in schizophrenia, expanding cohort sizes dilutes the aetiological effect of multiple individual variations. In our studies, we were able to identify a relatively a small subgroup of schizophrenics for which idiopathic carbonyl stress is a probable causative factor, from the heterogeneous schizophrenia population. This was achieved by applying our findings from a prototypic case carrying a frameshift mutation of *GLO1* and showing extremely high plasma AGEs, along with markedly low serum vitamin B_6 levels, to general patients. Within our hypothesis, elevated

Table 1 | Association between the *GLO1* genotype and carbonyl stress
χ^2 = 7.727; degrees of freedom = 1; P = 0.0054; odds ratio = 5.632; 95% confidence interval = 1.466–2164.

	AGEs	
GLO1 genotype	High	Normal
Frameshift, Ala/Ala	9 (4.5%)	3 (1.5%)
Glu/Ala, Glu/Glu	57 (28.5%)	107 (53.5%)

plasma AGEs and concomitant low vitamin B_6 levels could represent the most cogent and easily measurable 'biomarkers' in schizophrenia, and ultimately form the basis for the classification of heterogeneous types of schizophrenia based on biological causes.

As an individual marker, depleted vitamin B_6 might reflect elevated carbonyl stress induced by Glo1 defects and other as yet unknown cascades in schizophrenics. If carbonyl stress induces the development of schizophrenia and its symptoms, it is logical to assume that agents able to inhibit AGEs formation or entrap carbonyl compounds could provide therapeutic benefit to this subset of patients. There are currently a number of AGE-inhibitory compounds available for clinical use, such as angiotensin receptor blockers. In addition, compounds such as pyridoxamine and TM2002 possess potent ability to entrap toxic carbonyl compounds and prevent toxicity. In particular, schizophrenic patients with markedly lowered vitamin B_6 and high pentosidine levels may well benefit from treatment with pyridoxamine, a non-toxic water-soluble form of vitamin B_6. As mentioned above, non-psychotic subjects carrying a frameshift mutation in *GLO1* showed normal plasma AGEs and vitamin B_6 levels. They also exhibited significantly higher plasma glutathione and zinc concentrations compared with schizophrenics harbouring the mutation. This finding highlights both of these substrates as natural and safe therapeutic agents for patients with idiopathic carbonyl stress.

The symptoms of schizophrenia are usually classified into one of two categories: positive symptoms which represent a change in behaviour or thoughts, typified by hallucinations or delusions, and negative symptoms which represent a withdrawal or absence of the functions usually expected in healthy subjects. These patients often appear emotionless, flat and apathetic. Most anti-psychotic medications are effective for positive, but not negative, symptoms. We assessed the symptom severity of schizophrenics showing idiopathic carbonyl stress, using PANSS (Positive and Negative Syndrome Scale) [37]. We compared PANSS with plasma levels of AGEs. Although positive symptoms showed no correlation with AGEs, negative symptoms correlated significantly with AGE levels. It is therefore highly plausible that therapeutic inhibition of AGEs may improve negative symptoms. As a suppressor of idiopathic carbonyl stress, pyridoxamine could represent a very attractive medication for improving negative symptoms in this subset of schizophrenics.

Conclusion

Idiopathic carbonyl stress, typified by elevated AGE levels, occurs in a subpopulation of schizophrenics who show no evidence of diabetes mellitus and renal dysfunction. In the present review, we have described findings which suggest that Glo1 deficits and carbonyl stress are linked to the development of a subset of schizophrenia, and show a correlation with the severity of negative symptoms. Elevated plasma pentosidine and concomitant lowered vitamin B_6 levels may provide the most cogent and easily measurable 'biomarkers' in schizophrenia. They could also form the basis for classifying heterogeneous types of schizophrenia, according to their biological causes. Q1

References

1 Sullivan, P.F., Kendler, K.S. and Neale, M.C. (2003) Schizophrenia as a complex trait: evidence from a meta-analysis of twin studies. Arch. Gen. Psychiatry **60**, 1187–1192
2 Sullivan, P.F. (2005) The genetics of schizophrenia. PLoS Med. **2**, e212
3 Schulz, J.B., Lindenau, J., Seyfried, J. and Dichgans, J. (2000) Glutathione, oxidative stress and neurodegeneration. Eur. J. Biochem. **267**, 4904–4911
4 Tosic, M., Ott, J., Barral, S., Bovet, P., Deppen, P., Gheorghita, F., Matthey, M.L., Parnas, J., Preisig, M., Saraga, M. et al. (2006) Schizophrenia and oxidative stress: glutamate cysteine ligase modifier as a susceptibility gene. Am. J. Hum. Genet. **79**, 586–592
5 Young, J., McKinney, S.B., Ross, B.M., Wahle, K.W. and Boyle, S.P. (2007) Biomarkers of oxidative stress in schizophrenic and control subjects. Prostaglandins Leukot. Essent. Fatty Acids **76**, 73–85
6 Ng, F., Berk, M., Dean, O. and Bush, A.I. (2008) Oxidative stress in psychiatric disorders: evidence base and therapeutic implications. Int. J. Neuropsychopharmacol. **11**, 851–876
7 Thornalley, P.J. (1993) The glyoxalase system in health and disease. Mol. Aspects Med. **14**, 287–371
8 Brown, A.S., Bottiglieri, T., Schaefer, C.A., Quesenberry, Jr, C.P., Liu, L., Bresnahan, M. and Susser, E.S. (2007) Elevated prenatal homocysteine levels as a risk factor for schizophrenia. Arch. Gen. Psychiatry **64**, 31–39
9 Frankenburg, F.R. (2007) The role of one-carbon metabolism in schizophrenia and depression. Harv. Rev. Psychiatry **15**, 146–160
10 Gilbody, S., Lewis, S. and Lightfoot, T. (2007) Methylenetetrahydrofolate reductase (MTHFR) genetic polymorphisms and psychiatric disorders: a HuGE review. Am. J. Epidemiol. **165**, 1–13
11 Gysin, R., Kraftsik, R., Sandell, J., Bovet, P., Chappuis, C., Conus, P., Deppen, P., Preisig, M., Ruiz, V., Steullet, P. et al. (2007) Impaired glutathione synthesis in schizophrenia: convergent genetic and functional evidence. Proc. Natl. Acad. Sci. U.S.A. **104**, 16621–16626
12 Haidemenos, A., Kontis, D., Gazi, A., Kallai, E., Allin, M. and Lucia, B. (2007) Plasma homocysteine, folate and B_{12} in chronic schizophrenia. Prog. Neuropsychopharmacol. Biol. Psychiatry **31**, 1289–1296
13 Levine, J., Stahl, Z., Sela, B.A., Ruderman, V., Shumaico, O., Babushkin, I., Osher, Y., Bersudsky, Y. and Belmaker, R.H. (2006) Homocysteine-reducing strategies improve symptoms in chronic schizophrenic patients with hyperhomocysteinemia. Biol. Psychiatry **60**, 265–269
14 Saadat, M., Mobayen, F. and Farrashbandi, H. (2007) Genetic polymorphism of glutathione S-transferase T1: a candidate genetic modifier of individual susceptibility to schizophrenia. Psychiatry Res. **153**, 87–91
15 Yao, J.K., Leonard, S. and Reddy, R. (2006) Altered glutathione redox state in schizophrenia. Dis. Markers **22**, 83–93
16 Kirk, R.L., Theophilus, J., Whitehouse, S., Court, J. and Zimmet, P. (1979) Genetic susceptibility to diabetes mellitus: the distribution of properdin factor B (Bf) and glyoxalase (GLO) phenotypes. Diabetes **28**, 949–951
17 Miyata, T., van Ypersele de Strihou, C., Imasawa, T., Yoshino, A., Ueda, Y., Ogura, H., Kominami, K., Onogi, H., Inagi, R., Nangaku, M. and Kurokawa, K. (2001) Glyoxalase I deficiency is associated with an unusual level of advanced glycation end products in a hemodialysis patient. Kidney Int. **60**, 2351–2359
18 Fujimoto, M., Uchida, S., Watanuki, T., Wakabayashi, Y., Otsuki, K., Matsubara, T., Suetsugi, M., Funato, H. and Watanabe, Y. (2008) Reduced expression of glyoxalase-1 mRNA in mood disorder patients. Neurosci. Lett. **438**, 196–199
19 Junaid, M.A., Kowal, D., Barua, M., Pullarkat, P.S., Sklower Brooks, S. and Pullarkat, R.K. (2004) Proteomic studies identified a single nucleotide polymorphism in glyoxalase I as autism susceptibility factor. Am. J. Med. Genet. A **131**, 11–17
20 Sacco, R., Papaleo, V., Hager, J., Rousseau, F., Moessner, R., Militerni, R., Bravaccio, C., Trillo, S., Schneider, C., Melmed, R. et al. (2007) Case-control and family-based association studies of candidate genes in autistic disorder and its endophenotypes: *TPH2* and *GLO1*. BMC Med. Genet. **8**, 11

21 Politi, P., Minoretti, P., Falcone, C., Martinelli, V. and Emanuele, E. (2006) Association analysis of the functional Ala111Glu polymorphism of the glyoxalase I gene in panic disorder. Neurosci. Lett. **396**, 163–166
22 Ledig, M., Doffoel, M., Ziessel, M., Kopp, P., Charrault, A., Tongio, M.M., Mayer, S., Bockel, R. and Mandel, P. (1986) Frequencies of glyoxalase I phenotypes as biological markers in chronic alcoholism. Alcohol **3**, 11–14
23 Ditzen, C., Jastorff, A.M., Kessler, M.S., Bunck, M., Teplytska, L., Erhardt, A., Krömer, S.A., Varadarajulu, J., Targosz, B.S., Sayan-Ayata, E.F. et al. (2006) Protein biomarkers in a mouse model of extremes in trait anxiety. Mol. Cell. Proteomics **5**, 1914–1920
24 Hovatta, I., Tennant, R.S., Helton, R., Marr, R.A., Singer, O., Redwine, J.M., Ellison, J.A., Schadt, E.E., Verma, I.M., Lockhart, D.J. and Barlow, C. (2005) Glyoxalase 1 and glutathione reductase 1 regulate anxiety in mice. Nature **438**, 662–666
25 Krömer, S.A., Kessler, M.S., Milfay, D., Birg, I.N., Bunck, M., Czibere, L., Panhuysen, M., Pütz, B., Deussing, J.M., Holsboer, F. et al. (2005) Identification of glyoxalase-I as a protein marker in a mouse model of extremes in trait anxiety. J. Neurosci. **25**, 4375–4384
26 Arolt, V., Lencer, R., Nolte, A., Müller-Myhsok, B., Purmann, S., Schürmann, M., Leutelt, J., Pinnow, M. and Schwinger, E. (1996) Eye tracking dysfunction is a putative phenotypic susceptibility marker of schizophrenia and maps to a locus on chromosome 6p in families with multiple occurrence of the disease. Am. J. Med. Genet. **67**, 564–579
27 Brzustowicz, L.M., Honer, W.G., Chow, E.W., Hogan, J., Hodgkinson, K. and Bassett, A.S. (1997) Use of a quantitative trait to map a locus associated with severity of positive symptoms in familial schizophrenia to chromosome 6p. Am. J. Hum. Genet. **61**, 1388–1396
28 Nurnberger, Jr, J.I. and Foroud, T. (1999) Chromosome 6 workshop report. Am. J. Med. Genet. **88**, 233–238
29 Turner, W.J. (1979) Genetic markers for schizotaxia. Biol. Psychiatry **14**, 177–206
30 Arai, M., Yuzawa, H., Nohara, I., Ohnishi, T., Obata, N., Iwayama, Y., Haga, S., Toyota, T., Ujike, H., Arai, M. et al. (2010) Enhanced carbonyl stress in a subpopulation of schizophrenia. Arch. Gen. Psychiatry **67**, 589–597
31 Arai, M., Koike, S., Oshima, N., Takizawa, R., Araki, T., Miyashita, M., Nishida, A., Miyata, T., Kasai, K. and Itokawa, M. (2011) Idiopathic carbonyl stress in a drug-naive case of at-risk mental state. Psychiatry Clin. Neurosci. **65**, 606–607
32 Steinberg, S., de Jong, S., Mattheisen, M., Costas, J., Demontis, D., Jamain, S., Pietiläinen, O.P., Lin, K., Papiol, S., Huttenlocher, J. et al. (2014) Common variant at 16p11.2 conferring risk of psychosis. Mol. Psychiatry **19**, 108–114
33 Shi, J., Levinson, D.F., Duan, J., Sanders, A.R., Zheng, Y., Pe'er, I., Dudbridge, F., Holmans, P.A., Whittemore, A.S., Mowry, B.J. et al. (2009) Common variants on chromosome 6p22.1 are associated with schizophrenia. Nature **460**, 753–757
34 Stefansson, H., Ophoff, R.A., Steinberg, S., Andreassen, O.A., Cichon, S., Rujescu, D., Werge, T., Pietiläinen, O.P., Mors, O., Mortensen, P.B. et al. (2009) Common variants conferring risk of schizophrenia. Nature **460**, 744–747
35 Stefansson, H., Rujescu, D., Cichon, S., Pietiläinen, O.P., Ingason, A., Steinberg, S., Fossdal, R., Sigurdsson, E., Sigmundsson, T., Buizer-Voskamp, J.E. et al. (2008) Large recurrent microdeletions associated with schizophrenia. Nature **455**, 232–236
36 Manolio, T.A., Rodriguez, L.L., Brooks, L., Abecasis, G., Ballinger, D., Daly, M., Donnelly, P., Faraone, S.V., Frazer, K., Gabriel, S. et al. (2007) New models of collaboration in genome-wide association studies: the Genetic Association Information Network. Nat. Genet. **39**, 1045–1051
37 Kay, S.R. (1990) Positive-negative symptom assessment in schizophrenia: psychometric issues and scale comparison. Psychiatr. Q. **61**, 163–178

Received 18 February 2014
doi:10.1042/BST20140044

Measurement of glyoxalase activities

Makoto Arai*†[1], Naomi Nihonmatsu-Kikuchi*†, Masanari Itokawa†, Naila Rabbani* and Paul J. Thornalley*[1]

*Clinical Sciences Research Laboratories, Warwick Medical School, University of Warwick, University Hospital, Coventry CV2 2DX, U.K.

†Department of Psychiatry and Behavioral Sciences, Tokyo Metropolitan Institute of Medical Science, Tokyo 156-8506, Japan

Abstract

Glyoxalase 1 catalyses the isomerization of the hemithioacetal formed non-enzymatically from methylglyoxal and glutathione to *S*-D-lactoylglutathione. The activity of glyoxalase 1 is conventionally measured spectrophotometrically by following the increase in A_{240} for which the change in molar absorption coefficient $\Delta\varepsilon_{240} = 2.86\ mM^{-1}\cdot cm^{-1}$. The hemithioacetal is pre-formed *in situ* by incubation of methylglyoxal and glutathione in 50 mM sodium phosphate buffer (pH 6.6) at 37°C for 10 min. The cell extract is then added, the A_{240} is monitored over 5 min, and the initial rate of increase in A_{240} and hence glyoxalase 1 activity deduced with correction for blank. Glyoxalase 1 activity is given in units per mg of protein or cell number where one unit is the amount of enzyme that catalyses the formation of 1 μmol of *S*-D-lactoylglutathione per min under assay conditions. Glyoxalase 2 catalyses the hydrolysis of *S*-D-lactoylglutathione to D-lactate and glutathione. Glyoxalase 2 activity is also measured spectrophotometrically by following the decrease in A_{240} for which the change in molar absorption coefficient $\Delta\varepsilon_{240} = -3.10\ mM^{-1}\cdot cm^{-1}$. It is given in units per mg of protein or cell number where one unit is the amount of enzyme that catalyses the hydrolysis of 1 μmol of *S*-D-lactoylglutathione per min under assay conditions. Glyoxalase 1 and glyoxalase 2 activity measurements have been modified for use with a UV-transparent microplate for higher sample throughput.

Introduction

MG (methylglyoxal) is a reactive α-oxoaldehyde metabolite formed by the degradation of the triosephosphates glyceraldehyde 3-phosphate and dihydroxyacetone phosphate by MG synthase in bacteria, oxidation of acetone formed in ketone body metabolism, catabolism of threonine and degradation of glycated proteins [1]. MG is a reactive glycating agent and precursor of major quantitative AGE (advanced glycation end-product) adducts formed from protein and DNA. MG accumulation produces activation and increased degradation of proteins, DNA strand breaks, mutagenesis and cytotoxicity [2,3]. Protein and DNA damage is prevented by the efficient metabolism and detoxification of MG. The major pathway of MG metabolism is usually the glyoxalase pathway, supported by aldo–keto reductases (including aldose reductase) and aldehyde dehydrogenases [4,5].

The glyoxalase system is present in the cytosol of all mammalian cells and most organisms. Where it is absent, MG metabolism is achieved by aldo–keto reductases and aldehyde dehydrogenases. In the glyoxalase pathway, in the first step Glo1 (glyoxalase I) catalyses the isomerization of the HA (hemithioacetal) formed non-enzymatically from MG and reduced glutathione (GSH) to SLG (*S*-D-lactoylglutathione). In the second step, Glo2 (glyoxalase II) catalyses the hydrolysis of SLG to D-lactate and GSH, reforming GSH consumed in the Glo1-catalysed reaction.

Key words: glutathione, glyoxalase, high-throughput microplate assay, methylglyoxal, spectrophotometer.

Abbreviations: AG, aminoguanidine; Glo, glyoxalase; HA, hemithioacetal; MG, methylglyoxal; SLG, *S*-D-lactoylglutathione.

[1]Correspondence may be addressed to either of these authors (email arai-mk@igakuken.or.jp or P.J.Thornalley@warwick.ac.uk).

Recent studies implicate the glyoxalase pathway in human aging and disease, plant and microbial growth, resistance to drug therapy and environmental stress. Increased activity of Glo1 through gene copy number variation, regulation of transcriptional control and small-molecule inducers is now being investigated for improved understanding of mechanisms and pharmacological interventions to sustain healthy aging and for treatment of disease. Cell-permeant Glo1 inhibitors are also in development for treatment of multidrug resistance in cancer chemotherapy [6,7]. A one-step high-throughput microplate assay will be useful for screening of bioactives and drugs to improve and correct dysfunction of glyoxalase activity. This rapid and simple method will be also useful in elucidating the cellular and molecular mechanisms of glyoxalase metabolism.

Measurement of Glo1 and Glo2 activity using spectrophotometric assays

Sample preparation

The activities of Glo1 and Glo2 are made on cytosolic extracts of animal and plant tissues and extracts of animal, plant and microbial cells. Samples should be stored at −80°C if analysis cannot be performed immediately. Sample storage validation was reported previously [8]. The extract is conveniently prepared by homogenizing tissue in 10 mM sodium phosphate buffer (pH 7.0) or lysing washed cells in the same buffer by sonication. The homogenate or cell lysate is centrifuged to sediment membranes and the supernatant is the cytosolic extract used for assay of Glo1 and

Glo2 activities. With appropriate subcellular fractionation, activity of Glo2 in mitochondria may also be measured [9]. The cell number of cultured cells is counted before sonication if the activities of Glo1 and Glo2 are to be normalized to cell number (per million cells). Also, cells must be washed three times in PBS before sonication to remove extracellular protein from culture medium to allow for assay of cell protein and normalization of the activities of Glo1 and Glo2 to cell protein (mg). Total cell protein content is determined by Bradford assay or other method. Tissue and cells may also be lysed in a commercial lysis buffer containing protease inhibitors in accordance with the manufacturer's procedures. For example, Lysis-M buffer (Roche) containing a Complete™ mini EDTA-free protease inhibitor cocktail tablet and phosphatase inhibitor cocktail tablet.

Assay of activity of Glo1

The activity of Glo1 is measured spectrophotometrically using 1 ml quartz cuvettes by following the initial rate of increase in A_{240} for which the change in molar absorption coefficient $\Delta\varepsilon_{240}$ ($\Delta\varepsilon_{240} = \varepsilon_{240}[SLG] - \varepsilon_{240}[HA]$) = 2.86 $mM^{-1}\cdot cm^{-1}$ [10]. A blank correction is required. This should give a very low rate of increase in A_{240} (approximately <0.001 absorbance units per min). If the blank is higher, it may indicate contamination of the cuvette with Glo1 from a previous assay. In this case, clean the cuvettes with concentrated nitric acid, wash with 10 volumes of water and repeat the assay.

HA is pre-formed by incubation of 2 mM MG and 2 mM GSH in 50 mM sodium phosphate buffer (pH 6.6) at 37°C for 10 min ([HA] = 0.63 mM; $K = 333\ M^{-1}$ [11]). It must be pre-formed or the activity assay may be rate-limited by the rate of the HA formation and not Glo1 in the assay mixture. The HA solution should be freshly prepared and not be prepared in large volumes beforehand as it will slowly isomerize to *S*-lactoylglutathione non-enzymatically [12].

$\Delta\varepsilon_{240}$ for the Glo1 activity assay relates to the ε_{240} of SLG and HA and not to that of GSH and MG because, under the initial rate conditions, HA is converted into SLG before the equilibrium involving GSH and GSH relaxes under the new concentration conditions. The activity of Glo1 may be assayed by the accumulation of SLG even with cell extracts containing Glo2 because, under the assay conditions, the high concentration of HA used is a competitive inhibitor of Glo2 [13].

High-purity aqueous solution of MG, prepared and purified as described in [14], should preferably be used in the assay. MG stock solutions must be calibrated before use. This can be conveniently done by derivatization with AG (aminoguanidine). A small aliquot of MG solution is diluted to approximately 50–100 μM in a solution containing 1 mM AG hydrochloride in 50 mM sodium phosphate buffer (pH 7.4), with incubation at 37°C for 4 h and spectrophotometric measurement of the triazine adduct at 320 nm from which the concentration of MG is deduced (ε_{320} = 2411 $mM^{-1}\cdot cm^{-1}$) [15].

Assay of activity of Glo2

The activity of Glo2 is measured spectrophotometrically using 1 ml quartz cuvettes by following the initial rate of decrease in A_{240} for which the change in molar absorption coefficient $\Delta\varepsilon_{240}$ ($\Delta\varepsilon_{240} = \varepsilon_{240}$[D-lactic acid] + $\varepsilon_{240}[GSH] - \varepsilon_{240}[SLG]$) = $-3.10\ mM^{-1}\cdot cm^{-1}$ [10]. A blank correction is required. This should give a very low rate of increase in A_{240} (approximately <0.001 absorbance units per min). If the blank is higher, it may indicate contamination of the cuvette with Glo2 from a previous assay. In this case, clean the cuvettes with concentrated nitric acid, wash with 10 volumes of water and repeat the assay.

SLG stock solution should be calibrated before use as described. The concentration of SLG is determined by end point assay involving hydrolysis to D-lactate and GSH, catalysed by authentic Glo2. An aliquot of the stock solution of SLG (100 μl), Tris/HCl (pH 7.4) (100 mM, 500 μl) and water (390 μl) is added to a 1 ml quartz cuvette and the A_{240} is measured against a reference cuvette containing Tris/HCl (pH 7.4) (100 mM, 500 μl) and water (490 μl) at 37°C. Glo2 (100 units/ml, 10 μl) is added to the assay and reference cuvettes and the A_{240} is monitored until a steady minimum is attained. The concentration of SLG is deduced from the decrease in A_{240} on addition of Glo2; $\Delta\varepsilon_{240}$ = $-3.10\ mM^{-1}\cdot cm^{-1}$ [10].

Sample preparation of cell lysates and measurement of enzymatic activity by high-throughput microplate assay

Samples are analysed as above except absorbance measurements are made with UV-transparent 96-well microplates and reagent and cell extract volumes decreased 4- or 5-fold for 250 μl or 200 μl final assay mixture volumes. The change in absorption coefficients no longer apply as they are for 1 nm bandwidth and measurements made with 1 cm light pathlength. In the microplate reader, the bandwidth is typically 10 nm and the light pathlength approximately 0.4–0.5 cm. The change in absorption coefficients can be deduced by determined specific absorbance for reaction reagents and products in the Glo1 and Glo2 reactions in the microplate readers for wavelength-specific filter or monochromator bandwidths and pathlengths used. We have used 96-well flat-bottomed UV-transparent microplates (Corning), multichannel pipette and plate reader (FLUOstar OPTIMA, BMG Labtech) for measuring enzymatic activity of cell lysates for high-throughput. The A_{240} was followed by reading the absorbance of samples every 1 min for 20 min at 37°C. For optimal assay conditions of Glo1 activity, we found that 4 μg of sample proteins per well gives a measurable and linear increase in absorbance over 10 min of incubation, although this depends on the specific Glo1 activity of the sample.

Comparison with older protocols

In early periods of glyoxalase research, imidazole buffer, often supplemented with Mg^{2+} ions, was used for the measurement

Table 1 | Protocol for assay of activities of Glo1 and Glo2 Q1

For microplate assay, decrease reagent and cell extract volumes by a factor of 4 or 5 for total well volumes of 250 μl or 200 μl respectively.

Step	Description	Procedure
1	Preparation of biological samples	Animal and plant tissue: tissue (~5–10 mg of wet weight) is homogenized in 200 μl of 10 mM sodium phosphate buffer (pH 7.0) at 4°C. Cultured cells: cell pellets (~1×10^6) are washed three times in PBS, suspended in 200 μl of 10 mM sodium phosphate buffer (pH 7.0) at 4°C and sonicated at 100 W for 30 s. Cell fibrils and membranes are sedimented by centrifugation at 20000 ***g*** for 30 min at 4°C and the supernatant is removed and kept on ice for activity assays or stored at −80°C until analysis
2	Substrate solutions	Glo1 activity assay solutions required: 100 mM sodium phosphate buffer (pH 6.6) at 37°C, 20 mM GSH (hydrochloride salt) in water on ice, 20 mM MG in water on ice (calibrated by the AG method, see above) and water at 37°C. Glo2 activity assay solutions required: 100 mM Tris/HCl (pH 7.4) at 37°C, 3 mM SLG (calibrated spectrophotometrically) and water at 37°C
3	Assay of Glo1 activity	In a 1 ml cuvette, add 500 μl of 100 mM sodium phosphate buffer (pH 6.6) at 37°C, 100 μl of 20 mM GSH solution, 100 μl of 20 mM MG and 280 μl of water. The mixture is then incubated for 10 min at 37°C. After 10 min, 20 μl of cytosolic tissue/cell extract is added and the A_{240} is monitored immediately for 5 min. The initial rate of change (increases) in A_{240} is deduced, $(dA_{240}/dt)_0$, and the activity of Glo1 (units), a_{Glo1}, is deduced: $a_{Glo1} = (dA_{240}/dt)_0/2.86$
4	Assay of Glo2 activity	In a 1 ml cuvette, add 500 μl of 100 mM Tris/HCl (pH 7.4) at 37°C, 100 μl of 3 mM SLG solution and 350 μl of water. Then, 20 μl of cytosolic tissue/cell extract is added, and the A_{240} is monitored immediately for 5 min. The initial rate of change (decreases) in A_{240} is deduced, $(dA_{240}/dt)_0$, and the activity of Glo2 (units), a_{Glo2}, is deduced: $a_{Glo2} = -(dA_{240}/dt)_0/3.10$
5	Normalization	a_{Glo1} and a_{Glo2} are reported normalized to cell protein, assayed in the cytosolic extract or cell number (counted before cell lysis), as units/mg of protein or units/10^6 cells

of Glo1 activity; for example, 7.9 mM MG, 1 mM GSH, 14.6 mM $MgSO_4$ and 182 mM imidazole/HCl (pH 7.0) [16]. Imidazole buffer should not be used as it catalysis the isomerization of HA to *S*-lactoylglutathione [12]. Magnesium salts are not required and very high concentrations of MG are to be avoided as they will produce some inhibition of Glo1. When kinetic constants of Glo1 are to be determined, for example Michaelis–Menten constant K_m and enzyme turnover k_{cat}, the concentration of the HA substrate should be computed from the equilibrium constant of HA formation (333 M^{-1} [11]), maintaining a relative low and constant concentration of GSH at equilibrium, for example 1 mM, as GSH is a competitive inhibitor of Glo1 ($K_i = 8$ mM) [1].

It has been noted in some recent studies that phosphate buffer may be a weak inhibitor of Glo1 and approximately 10% higher activity was obtained by using Mops buffer instead [17,18]. We did not find this in lysates of human cells in culture, but it may be worth trying in particular samples of interest.

The activity of Glo1 and Glo2 may be measured with other substrates, such as glyoxal, hydroxypyruvaldehyde and phenylglyoxal. When this is desired, appropriate values for $\Delta\varepsilon_{240}$ may be deduced from the $\Delta\varepsilon_{240}$ of *S*-glycolylglutathione, *S*-L-glyceroylglutathione and *S*-D-mandelylglutathione [10].

Assessment for effect of bioactives and drugs on Glo1 activity by microplate assay

For an *in vitro* bioassay, it is important to establish a more simple, rapid and quantitative high-throughput method. The microplate-based method provides this (Table 2). It is a suitable method for simply and rapidly measuring large numbers of samples in screening bioactive and drug responses.

Table 2 | Comparison of two bioassay techniques for assessing glyoxalase activity

For Glo1 and Glo2 assay, avoid imidazole buffer and high concentrations of MG that inhibit glyoxalases.

Characteristic	Spectrophotometer-based assay	Microplate reader assay
Sample throughput	Low-throughput	Medium/high-throughput
Simplicity	Yes	Yes
Time required	15 min per sample	15 min per plate
Sensitivity	Moderate	Moderate
Quantitative	Yes	Yes
Consistency	Excellent ('gold standard')	Good

A one-step microplate assay was established for simple and rapid measurements of glyoxalase enzymatic activities in cell lysates. In addition, the assay in a large number of samples is possible and it will allow screening of bioactives that may up-regulate glyoxalase in the cells. The microplate method will be useful in elucidating the cellular and molecular mechanisms of glyoxalase metabolism, such as in metabolic function in cell and clinical samples [6,19].

Acknowledgements

We thank other members of host research teams for technical assistance: Dr Mingzhan Xue, Dr Jinit Masania, Dr Fozia Shaheen and Dr Attia Anwar.

Funding

This study was supported by a grant from Young Researcher Overseas Visits Program for Vitalizing Brain Circulation by Japan Society for the Promotion of Science (JSPS) fellowship: the collaborative study between Japan and the U.K. of molecular mechanisms of glycation and oxidative stress in psychiatric disorders.

References

1 Thornalley, P.J. (1993) The glyoxalase system in health and disease. Mol. Aspects Med. **14**, 287–371
2 Rabbani, N. and Thornalley, P.J. (2012) Methylglyoxal, glyoxalase 1 and the dicarbonyl proteome. Amino Acids **42**, 1133–1142
3 Thornalley, P.J., Waris, S., Fleming, T., Santarius, T., Larkin, S.J., Winklhofer-Roob, B.M., Stratton, M.R. and Rabbani, N. (2010) Imidazopurinones are markers of physiological genomic damage linked to DNA instability and glyoxalase 1-associated tumour multidrug resistance. Nucleic Acids Res. **138**, 5432–5442
4 Rabbani, N. and Thornalley, P.J. (2012) Dicarbonyls (glyoxal, methylglyoxal, and 3-deoxyglucosone). In Uremic Toxins (Niwa, T., ed.), pp. 177–192, John Wiley & Sons, Chichester
5 Rabbani, N., Xue, M. and Thornalley, P.J. (2014) Activity, regulation, copy number and function in the glyoxalase system. Biochem. Soc. Trans. **42**, xxx–xxx
6 Xue, M., Rabbani, N., Momiji, H., Imbasi, P., Anwar, M.M., Kitteringham, N.R., Park, B.K., Souma, T., Moriguchi, T., Yamamoto, M. and Thornalley, P.J. (2012) Transcriptional control of glyoxalase 1 by Nrf2 provides a stress responsive defence against dicarbonyl glycation. Biochem. J. **443**, 213–222
7 Thornalley, P.J. and Rabbani, N. (2011) Glyoxalase in tumourigenesis and multidrug resistance. Semin. Cell Dev. Biol. **22**, 318–325
8 McLellan, A.C. and Thornalley, P.J. (1992) Sample storage conditions for the assay of glyoxalase activities in whole blood samples. Ann. Clin. Biochem. **29**, 222–223
9 Talesa, V., Uotila, L., Koivusalo, M., Principato, G.B., Giovanni, E. and Rosi, G. (1988) Demonstration of glyoxalase II in rat liver mitochondria: partial purification and occurrence in multiple forms. Biochim. Biophys. Acta **955**, 103–110
10 Clelland, J.D. and Thornalley, P.J. (1991) *S*-2-hydroxyacylglutathione derivatives: enzymatic preparation, purification and characterisation. J. Chem. Soc. Perkin Trans. 1 **1991**, 3009–3015
11 Vander Jagt, D.L., Daub, F., Krohn, J.A. and Han, L.P. B. (1975) Effects of pH and thiols on the kinetics of yeast glyoxalase I: an evaluation of the random pathway mechanism. Biochemistry **14**, 3669–3675
12 Hall, S.S., Doweyko, A.M. and Jordan, F. (1978) Glyoxalase I enzyme studies. 4. General base catalysed enediol proton transfer rearrangement of methylglyoxal and phenylglyoxal-glutathionylhemithiol acetal to *S* lactoyl-*S* mandeloyl-glutathione followed by hydrolysis: a model for the glyoxalase system. J. Am. Chem. Soc. **100**, 5934–5939
13 Uotila, L. (1973) Purification and characterization of *S*-2-hydroxyacylglutathione from human liver. Biochemistry **12**, 3944–3951
14 McLellan, A.C. and Thornalley, P.J. (1992) Synthesis and chromatography of 1,2-diamino-4,5-dimethoxybenzene, 6,7-dimethoxy-2-methylquinoxaline and 6,7-dimethoxy-2,3-dimethylquinoxaline for use in a liquid chromatographic fluorimetric assay of methylglyoxal. Anal. Chim. Acta **263**, 137–142
15 Thornalley, P.J., Yurek-George, A. and Argirov, O.K. (2000) Kinetics and mechanism of the reaction of aminoguanidine with the α-oxoaldehydes, glyoxal, methylglyoxal and 3-deoxyglucosone under physiological conditions. Biochem. Pharmacol. **60**, 55–65
16 Oray, B. and Norton, S.J. (1980) Purification and characterization of mouse liver glyoxalase II. Biochim. Biophys. Acta **611**, 168–173
17 Suttisansanee, U., Lau, K., Lagishetty, S., Rao, K.N., Swaminathan, S., Sauder, J.M., Burley, S.K. and Honek, J.F. (2011) Structural variation in bacterial glyoxalase I enzymes: investigation of the metalloenzyme glyoxalase I from *Clostridium acetobutylicum*. J. Biol. Chem. **286**, 38367–38374
18 Deponte, M., Sturm, N., Mittler, S., Harner, M., Mack, H. and Becker, K. (2007) Allosteric coupling of two different functional active sites in monomeric *Plasmodium falciparum* glyoxalase I. J. Biol. Chem. **282**, 28419–28430
19 Arai, M., Yuzawa, H., Nohara, I. Ohnishi, T., Obata, N., Iwayama, Y., Haga, S., Toyota, T., Ujike, H., Arai, M. et al. (2010) Enhanced carbonyl stress in a subpopulation of schizophrenia. Arch. Gen. Psychiatry **67**, 589–597

Received 7 January 2014
doi:10.1042/BST20140010

SCIENTIFIC REPORTS

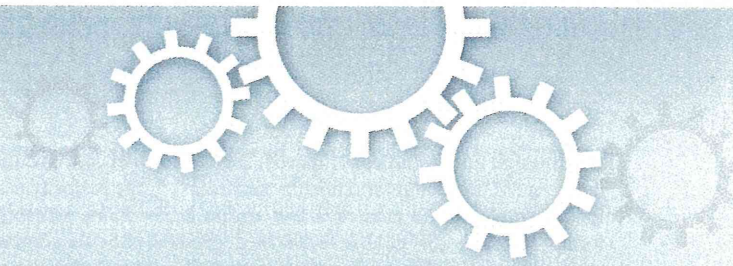

OPEN

SUBJECT AREAS:
BIOMARKER RESEARCH
DEPRESSION
DIAGNOSTIC MARKERS

Received
8 September 2014

Accepted
17 December 2014

Published
15 January 2015

Correspondence and requests for materials should be addressed to H.K. (hkunugi@ncnp.go.jp)

Reduced cerebrospinal fluid ethanolamine concentration in major depressive disorder

Shintaro Ogawa[1,7], Kotaro Hattori[1,2], Daimei Sasayama[1,3], Yuki Yokota[1,2], Ryo Matsumura[1,2], Junko Matsuo[1,7], Miho Ota[1], Hiroaki Hori[1], Toshiya Teraishi[1], Sumiko Yoshida[4], Takamasa Noda[4], Yoshiaki Ohashi[5], Hajime Sato[5], Teruhiko Higuchi[6], Nobutaka Motohashi[7] & Hiroshi Kunugi[1]

[1]Department of Mental Disorder Research, National Institute of Neuroscience, National Center of Neurology and Psychiatry, Kodaira, Tokyo, 187-8502, Japan, [2]Translational Medical Center, National Center of Neurology and Psychiatry, Kodaira, Tokyo, 187-8551, Japan, [3]Department of Psychiatry, Shinshu University School of Medicine, Matsumoto, Nagano, 390-8621, Japan, [4]Department of Psychiatry, National Center Hospital, National Center of Neurology and Psychiatry, Kodaira, Tokyo, 187-8551, Japan, [5]Human Metabolome Technologies, Inc., Tsuruoka, Yamagata, 997-0052, Japan, [6]National Center of Neurology and Psychiatry, Kodaira, Tokyo, 187-8551, Japan, [7]Department of Neuropsychiatry, Interdisciplinary Graduate School of Medicine and Engineering, University of Yamanashi, Chuo, Yamanashi, 409-3898, Japan.

Amino acids play key roles in the function of the central nervous system, and their alterations are implicated in psychiatric disorders. In the search for a biomarker for major depressive disorder (MDD), we used high-performance liquid chromatography to measure amino acids and related molecules in the cerebrospinal fluid (CSF) of 52 patients with MDD (42 depressed and 10 remitted; DSM-IV) and 54 matched controls. Significant differences were found in four amino acid concentrations between the depressed patients and controls. After Bonferroni correction, only ethanolamine (EA) levels remained significantly reduced in depressed patients (nominal $P = 0.0000011$). A substantial proportion of the depressed patients (40.5%) showed abnormally low CSF EA levels (<12.1 μM) ($P = 0.000033$; OR = 11.6, 95% CI: 3.1–43.2). When patients with low EA and those with high EA levels were compared, the former had higher scores for overall depression severity ($P = 0.0033$) and 'Somatic Anxiety' symptoms ($P = 0.00026$). In unmedicated subjects, CSF EA levels showed a significant positive correlation with levels of homovanillic acid ($P = 0.0030$) and 5-hydroxyindoleacetic acid ($P = 0.019$). To our knowledge, this is the first study showing that patients with MDD have significantly lower CSF EA concentrations compared with control subjects. CSF EA could be a state-dependent biomarker for a subtype of MDD.

Major depressive disorder (MDD) is a common disease with a prevalence rate estimated at 4.4% worldwide[1]. Since the pathophysiology of MDD remains elusive, no established biochemical marker is available for everyday use in the clinical setting and the diagnosis of MDD largely depends on the clinical interview[2]. Although many candidate molecules are present in peripheral blood[3], no study has successfully found a biomarker that is of practical use in the diagnosis, subtyping, or symptomatic assessment of MDD.

Since cerebrospinal fluid (CSF) contacts the interstitial fluid in the central nervous system (CNS)[4] and is mostly segregated from the peripheral circulation by the blood-brain barrier, CSF reflects molecular dynamics in the brain. The composition of CSF (electrolytes[5], amino acids[6], and proteins[7]) differs substantially from that of peripheral blood. Total tau and phosphorylated tau protein in CSF have been established as biomarkers for Alzheimer's disease[8], but are not detectable in peripheral blood. It is therefore feasible to search for a biomarker for MDD in the CSF. The proteomics approach to CSF samples seems to be promising[9].

We have focused on amino acids and related molecules in the CSF to identify a biomarker for MDD, because alterations in the serotonin, noradrenaline, dopamine, glutamate, and γ-amino-butyric acid (GABA) systems are implicated in MDD[10]. These neurotransmitters are themselves amino acids or are synthesized from amino acids. Previous studies examined amino acid levels in the peripheral blood of MDD patients, although their results are equivocal[11–14]. We have recently reported a meta-analysis demonstrating that the plasma L-tryptophan concentration is significantly lower in MDD patients than healthy controls ($P = 0.000059$)[15]. In this context, we chose to examine amino acids and related molecules in the CSF of MDD patients.

Although many studies compared CSF amino acid concentrations between MDD patients and healthy controls[16–28], the majority examined a single amino acid or a few amino acids. Some researchers found reduced CSF GABA levels in depressed patients compared with controls[18,19,21,28], while others reported contradictive negative results[17,20,22]. Increased glutamine levels in depressed patients[24], and reduced glutamate and glycine concentrations in refractory patients were reported[25], however, no differences in CSF glutamate and glutamine levels between 2 groups were inconsistently found[27]. No significant difference between patients and controls was found for tryptophan[21,23], tyrosine[21] or alanine[24]. To our knowledge, only two studies examined comprehensive amino acid profiles in CSF. An early study examined 32 amino acids and related molecules including ethanolamine (EA); however, that sample included only 8 subjects with unipolar depression and 2 controls[16]. A metabolomics-based approach in 14 currently-depressed patients, 14 remitted patients, and 18 controls found that CSF methionine levels were significantly increased in remitted patients compared with controls[26]. Thus, previous information on CSF amino acid levels in MDD patients is surprisingly limited.

We measured CSF amino acids and related molecules in a relatively large sample to search for a biomarker for MDD. We also analyzed the correlations between CSF amino acid levels and depression severity, psychotropic medication, and monoamine metabolites.

Subjects and methods

Subjects. Subjects were 52 patients with MDD and 54 healthy controls matched for age and sex. All participants were biologically-unrelated Japanese. Patients were recruited at the National Center of Neurology and Psychiatry (NCNP) Hospital (Tokyo, Japan), or through advertisements in free local magazines, and by our website. Healthy controls were from the same geographical area (i.e., western Tokyo metropolitan) via advertisements in magazines and website. Trained psychologists or psychiatrists conducted a structured Mini-International Neuropsychiatric Interview (M.I.N.I.)[29], Japanese version with all participants. A consensus diagnosis was made according to the Diagnostic and Statistical Manual of Mental Disorders, 4th edition (DSM-IV) criteria[30] based on the M.I.N.I., an additional unstructured interview, and information from medical records if available. Patients with any comorbid axis I disorder were excluded, as were individuals with a prior medical history of CNS disease, severe head injury, or substance abuse/dependence. After the nature of the study procedures had been fully explained, written informed consent was obtained from all subjects. MDD symptoms were assessed using the Japanese version of the 17-item Hamilton Depression Rating Scale (HAMD-17)[31], and the cut-off score for remission was ≤7[32]. Ten of the 52 patients were remitted. Among all MDD patients (depressed + remitted), 39 patients were medicated and the remaining 13 (11 depressed and 2 remitted) were not on psychotropic medication. Daily doses of benzodiazepine derivatives, antidepressants, and antipsychotics were converted to equivalent doses of diazepam, imipramine, and chlorpromazine respectively, using published guidelines[33] When each class of drugs was not medicated, the dose was considered to be zero. The present experiments on our participants were conducted in accordance with the Declaration of Helsinki. The study protocol was approved by the ethics committee at the NCNP (No. 305).

Sample collection. Between 10:00 h and 16:00 h, CSF samples were obtained by lumbar puncture from the L4–5 or L3–4 interspace of participants, in the left decubitus position. CSF samples were immediately placed on ice, and centrifuged at 4000 × *g*. Supernatants were aliquoted and stored at −80°C until assays were performed. All samples were collected from August 2010 to August 2013. Initial 2 mL of CSF was used for measuring glucose, chloride, total protein levels and monoamine metabolites. Homovanillic acid (HVA), 3-methoxy-4-hydroxyphenylethyleneglycol (MHPG), and 5-hydroxyindoleacetic acid (5-HIAA) were measured by high-performance liquid chromatography (HPLC) at SRL Co., Inc. (Tokyo, Japan).

Determination of CSF levels of amino acids and related molecules by HPLC. CSF sample was mixed with 4% 5-sulfosalicylic acid dihydrate (WAKO, Tokyo, Japan), and centrifuged for 10 min at 12,000 × *g* and 4°C. Each supernatant was transferred to a micro-tube, filtered using a 0.22-μm pore-diameter syringe-filter (AS ONE, Osaka, Japan), and subjected to HPLC (JASCO, Tokyo, Japan). Acquired data were processed and quantified on the chromatography data station ChromNAV (JASCO). A detailed description of the HPLC protocol is available in the Supplementary Methods.

Validation by capillary electrophoresis time-of-flight mass spectrometry (CE-TOF-MS). Amino acids and related molecules were also measured using CE-TOF-MS for a subset of the subjects (24 depressed, 3 remitted patients, and 27 controls). The CE-TOF-MS measurements were performed at Human Metabolome Technologies, Inc. (Yamagata, Japan), by coauthors who were blinded to the HPLC

Table 1 | Demographic and Clinical data on subjects

	dMDD	rMDD	HC	Statistics
N (Male/Female)	42 (19/23)	10 (6/4)	54 (28/26)	$\chi^2 = 0.86$, $df = 2$, $P = 0.63$ [1]
Age, year	45.5 ± 12.2	42.9 ± 14.9	43.6 ± 15.3	$F = 0.26$, $df = 2$, $P = 0.77$ [2]
BZD, mg/day (ratio)	14.1 ± 14.4 (29/42)	12.1 ± 17.9 (7/10)	N.A.	$t = 0.38$, $df = 50$, $P = 0.71$, 95% CI: −8.66 to 12.63 [3]
AD, mg/day (ratio)	136.9 ± 131.1 (27/42)	149.4 ± 170.4 (7/10)	N.A.	$t = -0.26$, $df = 50$, $P = 0.80$, 95% CI: −110.72 to 85.78 [3]
AP, mg/day (ratio)	83.7 ± 176.2 (13/42)	56.5 ± 125.5 (3/10)	N.A.	$t = 0.46$, $df = 50$, $P = 0.65$, 95% CI: −91.67 to 146.14 [3]
HAMD-17, score	18.0 ± 7.2	4.3 ± 2.4	N.A.	$t = 10.20$, $df = 44.93$, $P < 5 \times 10^{-13}$, 95% CI: 9.00 to 18.36 [3]
Time of CSF sampling, min [4]	185.2 ± 95.4	221.5 ± 111.9	172.2 ± 118.6	$F = 0.89$, $df = 2$, $P = 0.42$ [2]
Days from CSF sampling, day [5]	554.9 ± 313.5	721.5 ± 276.9	479.7 ± 286.4	$F = 3.01$, $df = 2$, $P = 0.054$ [2]

[1]Based on the chi-squared test with exact probability.
[2]Based on the analysis of variance.
[3]Based on the *t*-test.
[4]Sampling time is expressed as minutes from 10:00 AM.
[5]Number of days from the lumbar puncture day to Sep 1, 2013.
Abbreviations: dMDD, depressed (non-remitted) patients with major depressive disorder; rMDD, remitted patients; HC, healthy controls; HAMD-17, 17-item Hamilton Depression Rating Scale; CSF, cerebrospinal fluid; BZD, daily diazepam equivalent dose of benzodiazepine derivatives; AD, daily imipramine equivalent dose of antidepressants; AP, daily chrolpromazine equivalent dose of antipsycholics; CI, confidence interval for the difference between two means.

Table 2 | Comparisons between dMDD and HC for amino acids and related molecule profiles in cerebrospinal fluid

	dMDD ($N = 42$)		HC ($N = 54$)		Statistics for ANCOVA			
Name	μM ± *SD*	NMISS [1]	μM ± *SD*	NMISS	*F*	*df*	*P*	95% CI
Phosphoethanolamine	4.7 ± 1.2	0	5.1 ± 1.1	0	2.12	1	0.15	−0.75 to 0.11
Threonine	33.1 ± 9.3	0	29.8 ± 5.3	0	4.30	1	0.041	0.13 to 6.030
Serine	29.3 ± 7.5	0	27.9 ± 6.1	0	0.75	1	0.39	−1.51 to 3.86
Asparagine	7.2 ± 1.4	0	6.6 ± 1.3	0	3.85	1	0.053	−0.0065 to 1.11
Glutamine	711.3 ± 142.5	0	644.3 ± 108.8	0	6.70	1	0.011	15.16 to 115.15
Glycine	6.4 ± 2.0	0	6.0 ± 1.8	0	0.95	1	0.33	−0.38 to 1.12
Alanine	37.5 ± 10.3	0	33.7 ± 9.0	0	3.34	1	0.071	−0.31 to 7.47
α-Amino-n-butyric acid	2.7 ± 1.0	0	2.6 ± 0.9	0	0.30	1	0.59	−0.29 to 0.51
Valine	16.6 ± 4.8	0	15.2 ± 4.6	0	2.41	1	0.12	−0.39 to 3.23
Methionine	3.3 ± 0.9	0	3.5 ± 0.8	0	1.68	1	0.20	−0.56 to 0.12
Isoleucine	5.2 ± 1.5	0	4.8 ± 1.4	0	2.88	1	0.093	−0.080 to 1.017
Leucine	12.5 ± 3.4	0	11.5 ± 2.9	0	3.42	1	0.068	−0.082 to 2.27
Tyrosine	9.0 ± 1.8	0	9.4 ± 2.3	0	1.50	1	0.22	−1.34 to 0.32
Phenylalanine	10.1 ± 2.1	0	10.0 ± 2.3	0	0.038	1	0.85	−0.79 to 0.96
Ethanolamine	12.3 ± 2.3	0	14.8 ± 2.2	0	**27.36**	**1**	**0.0000011** [2]	**−3.29 to −1.48**
Lysine	24.3 ± 7.1	0	22.2 ± 3.9	0	3.11	1	0.081	−0.25 to 4.17
Histidine + 1-Methylhistidine	8.4 ± 2.7	0	8.0 ± 1.4	0	0.69	1	0.41	−0.50 to 1.21
Arginine	21.8 ± 5.1	0	22.6 ± 4.7	0	0.58	1	0.45	−2.79 to 1.25
Aspartate	0.7 ± 0.3	17	0.7 ± 0.2	21	1.091	1	0.30	−0.062 to 0.20
Glutamate	9.1 ± 5.4	2	8.3 ± 5.2	1	0.57	1	0.45	−1.39 to 3.088
Cystine	2.9 ± 0.7	6	2.8 ± 0.8	8	0.20	1	0.66	−0.25 to 0.40
Tryptophan	1.8 ± 0.7	19	2.0 ± 0.4	18	2.64	1	0.11	−0.55 to 0.058
Ornithine	2.9 ± 1.4	6	3.2 ± 1.5	7	1.52	1	0.22	−1.034 to 0.24
Carnosine	2.4 ± 1.5	7	3.3 ± 2.1	10	5.30	1	0.024	−1.58 to −0.11
γ-Aminobutyric acid	0.3 ± 0.1	24	0.3 ± 0.1	30	1.061	1	0.31	−0.023 to 0.072

[1]Missing values are replaced with blanks in the ANCOVA analysis.
[2]Adjusted significance was set at $P < 0.002$, and significant *P*-values after Bonferroni correction are in bold type.
Abbreviations: dMDD, depressed (non-remitted) patients with major depressive disorder; HC, healthy controls; SD, standard deviation; NMISS, number of missing values; ANCOVA, analysis of covariance; CI, confidence interval for the difference between two means.

data obtained at the NCNP. Compounds were identified by their peaks using annotated tables with *m/z* values and normalized by migration times. Detailed CE-TOF-MS procedures are described elsewhere[34].

Statistical analysis. Data are reported as means ± standard deviation (*SD*). Means were compared using *t*-tests or analysis of variance. Categorical variables were compared using the χ^2 test with exact probability. Analysis of covariance (ANCOVA), controlling for age and sex, was performed to compare CSF levels of amino acids and related molecules in the patients and controls and between subgroups of the patients. Partial correlation analysis, controlling for age and sex, was performed to examine the correlations between equivalent doses of psychotropic drugs and concentrations of amino acids and related molecules, and between EA levels and other CSF substances including biogenic amine metabolites. The Mann-Whitney *U* test with exact probability was used to compare clinical symptoms (HAMD-17 scores) between MDD subgroups (Low-EA vs. High-EA). We obtained 95% CI for the difference between two medians for Mann-Whitney *U* using Hodges-Lehmann estimate. HAMD-17 items were assigned to the following subscales: 'Core' (items 1, 2, 7, 8, 10, 13), 'Sleep' (items 4, 5, 6), 'Activity' (items 7, 8), 'Psychic Anxiety' (items 9, 10), and 'Somatic Anxiety' (items 11, 12, 13), according to Serretti *et al.*[35]. We used non-parametric estimate of receiver operating characteristic (ROC) curves for the assessment of specificity and sensitivity of EA to discriminate between MDD patients and controls, and between depressed and remitted MDD groups. Statistical significance for a two-tailed *P*-value was <0.05, and was corrected for multiple comparisons using the Bonferroni method. All analyses were performed using IBM SPSS Statistics 22.0 Japanese version (IBM Japan, Tokyo, Japan).

Results

Demographic and clinical characteristics of the subjects are shown in Table 1. There were no significant differences in sex ratio, age distribution, time of CSF sampling, or number or days from sample collection among the depressed, remitted, and control subjects. No significant difference was observed in psychotropic drug doses between depressed and remitted MDD groups. CSF concentrations of 25 of the 41 amino acids and related molecules were successfully determined in the majority of subjects (Table 2). There was nominally a significant difference in the concentrations of threonine, glutamine, EA, and carnosine between the depressed MDD and control groups. When the critical $P = 0.002$ (0.05/25) was conservatively applied after the Bonferroni correction, only EA remained significant (nominal $P = 0.0000011$).

We then performed detailed analyses on the possible relationships between CSF EA levels and clinical variables. In controls, there was no significant difference in CSF EA levels between men and women controlled for age ($F = 0.045$, $df = 1$, $P = 0.83$; 95% CI: −1.10 to 1.36), and no significant correlation between EA and age controlled for sex ($r = -0.063$, $df = 51$, $P = 0.66$; 95% CI: −0.33 to 0.21), between EA and time of CSF sampling controlled for sex and age ($r = 0.061$, $df = 50$, $P = 0.67$: 95% CI: −0.22 to 0.33), or between EA and number of days from sample collection controlled for sex and age ($r = 0.0062$, $df = 50$, $P = 0.97$; 95% CI: −0.27 to 0.28), in a partial correlation analysis. Figure 1a shows dot plots of CSF EA concentrations in depressed MDD patients and controls. Among all MDD patients, no significant difference in EA levels was observed between the medicated and unmedicated patients using ANCOVA, controlling for sex and age ($F = 0.0030$, $df = 1$, $P = 0.96$; 95%CI: −1.57 to 1.66) (Figure 1b), and there were no significant differences in age, sex, or total HAMD-17 score. When unmedicated MDD patients and controls were compared, there was a significant difference in CSF EA based on ANCOVA ($F = 7.0$, $df = 1$, $P = 0.010$; 95% CI: −3.28 to −0.46). Remitted MDD patients had significantly higher EA levels than depressed MDD patients (ANCOVA; $F = 8.1$, $df = 1$, $P = 0.0066$; 95%CI: 0.67 to 3.90) (Figure 1c), and they showed no significant differences in age or sex. There was no significant difference in CSF EA levels between remitted patients and controls ($F = 0.0092$, $df = 1$, $P = 0.92$; 95%CI: −1.68 to 1.53). These comparisons for CSF EA concentrations between subgroups are summarized in Table 3. Area under curve (AUC) by the ROC curve to discriminate between depressed (non-remitted) MDD patients and controls was 0.77 (Supplementary Fig. S1a), that between depressed and remitted MDD groups was 0.75 (Supplementary Fig. S1b), indicating 'fair test' for these discriminations. When "abnormally low CSF EA levels"

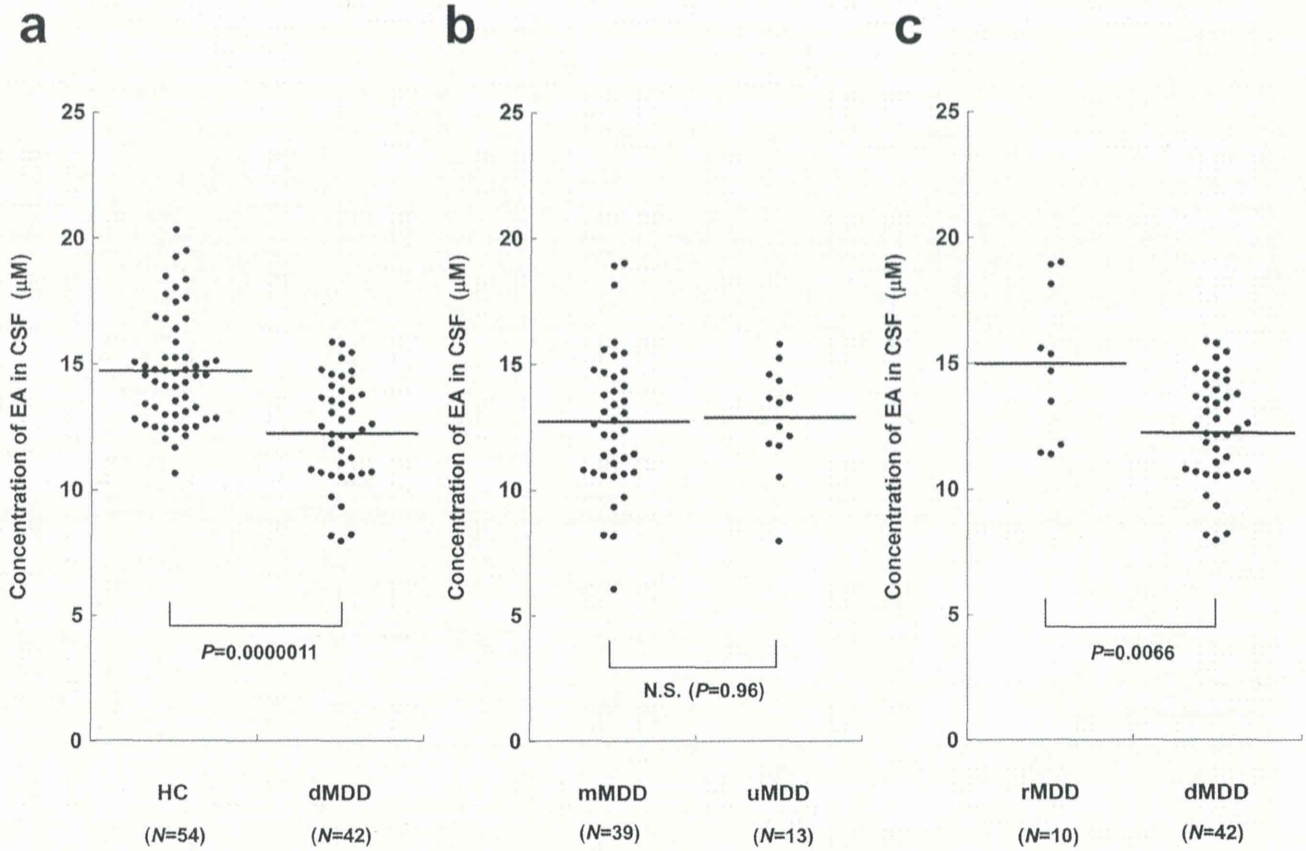

Figure 1 | Dot plots of CSF EA concentrations in patients with MDD and controls. Horizontal bars represent mean values of the groups. Statistical analyses were performed by ANCOVA, controlling for age and sex. (a) Comparison between dMDD patients and HC, (b) that between mMDD and uMDD, and (c) that between rMDD and dMDD. Abbreviations: CSF, cerebrospinal fluid; EA, ethanolamine; HC, healthy controls; dMDD, depressed (non-remitted) patients with major depressive disorder; rMDD, remitted patients; mMDD, medicated patients; uMDD, unmedicated patients; ANCOVA, analysis of covariance.

were defined as the 5th percentile value of the controls (<12.1 μM), 17 depressed patients (40.5%) and 3 controls fell within this range (χ^2 = 17.5, df = 1, P = 0.000033; OR = 11.6, 95% CI: 3.1 to 43.2).

To investigate the relationship between patient's symptoms and CSF EA levels, we defined MDD patients (depressed + remitted) whose levels fell below the 1st quartile of CSF EA values as 'Low-EA' (N = 13) and above the 3rd quartile as 'High-EA' (N = 13). The Low-EA group had higher HAMD-17 total scores (P = 0.0033, Mann-Whitney U test), and 'Core' (P = 0.034) and 'Somatic Anxiety' (P = 0.00026) subscale scores (Figure 2). Other HAMD subscales ('Sleep', 'Activity', and 'Psychic Anxiety') showed no significant differences between Low-EA and High-EA groups.

Although there was no significant difference in CSF EA levels between medicated and unmedicated MDD patients, we examined the possible correlation between the equivalent dose of psychotropic drugs and CSF amino acid levels in the depressed MDD group (Table S1). CSF EA levels did not significantly correlate with benzodiazepine derivatives (P = 0.29), antidepressants (P = 0.34), or antipsychotics (P = 0.21). With respect to other molecules, several amino acid concentrations nominally showed significant correlations with medications (Supplementary Table S1). The correlations between isoleucine and antidepressants (P = 0.00056) (Supplementary Fig. S2), remained significant even after correcting for multiple comparisons [critical P-value of 0.05/(25 × 2) = 0.001].

We further investigated the correlations between CSF EA levels and other CSF substances in unmedicated patients with MDD and controls (total N = 67), based on reports that levels of CSF biogenic amine metabolites are affected by psychotropic drugs[36]. HVA, a catabolite of dopamine (P = 0.0030), and 5-HIAA, a catabolite of serotonin (P = 0.019), showed significant correlations, while other substances (total protein, glucose, chloride, and MHPG) did not (Figure 3 and Table 4).

Table 3 | Summarized comparisons in CSF EA concentrations between subgroups

Comparisons	Differences	Statistics for ANCOVA [1]	95% CI
dMDD (N = 42) vs HC (N = 54)	12.3 ± 2.3 vs 14.8 ± 2.2	**F = 27.36, df = 1, P = 0.0000011**	**−3.29 to −1.48**
mMDD (N = 39) vs uMDD (N = 13)	12.8 ± 2.8 vs 12.9 ± 2.1	F = 0.0030, df = 1, P = 0.96	−1.57 to 1.66
dMDD (N = 42) vs rMDD (N = 10)	12.3 ± 2.3 vs 15.0 ± 3.0	**F = 8.073, df = 1, P = 0.0066**	**−3.90 to −0.67**

[1]Statistical values derived from ANCOVA controlling for sex and age.
Significant P-values are shown in bold type.
Abbreviations: CSF, cerebrospinal fluid; EA, ethanolamine; ANCOVA, analysis of covariance; dMDD, depressed (non-remitted) patients with major depressive disorder; rMDD, remitted patients; HC, healthy controls; uMDD, unmedicated patients; mMDD, medicated patients; CI, confidence interval for the difference between two means.

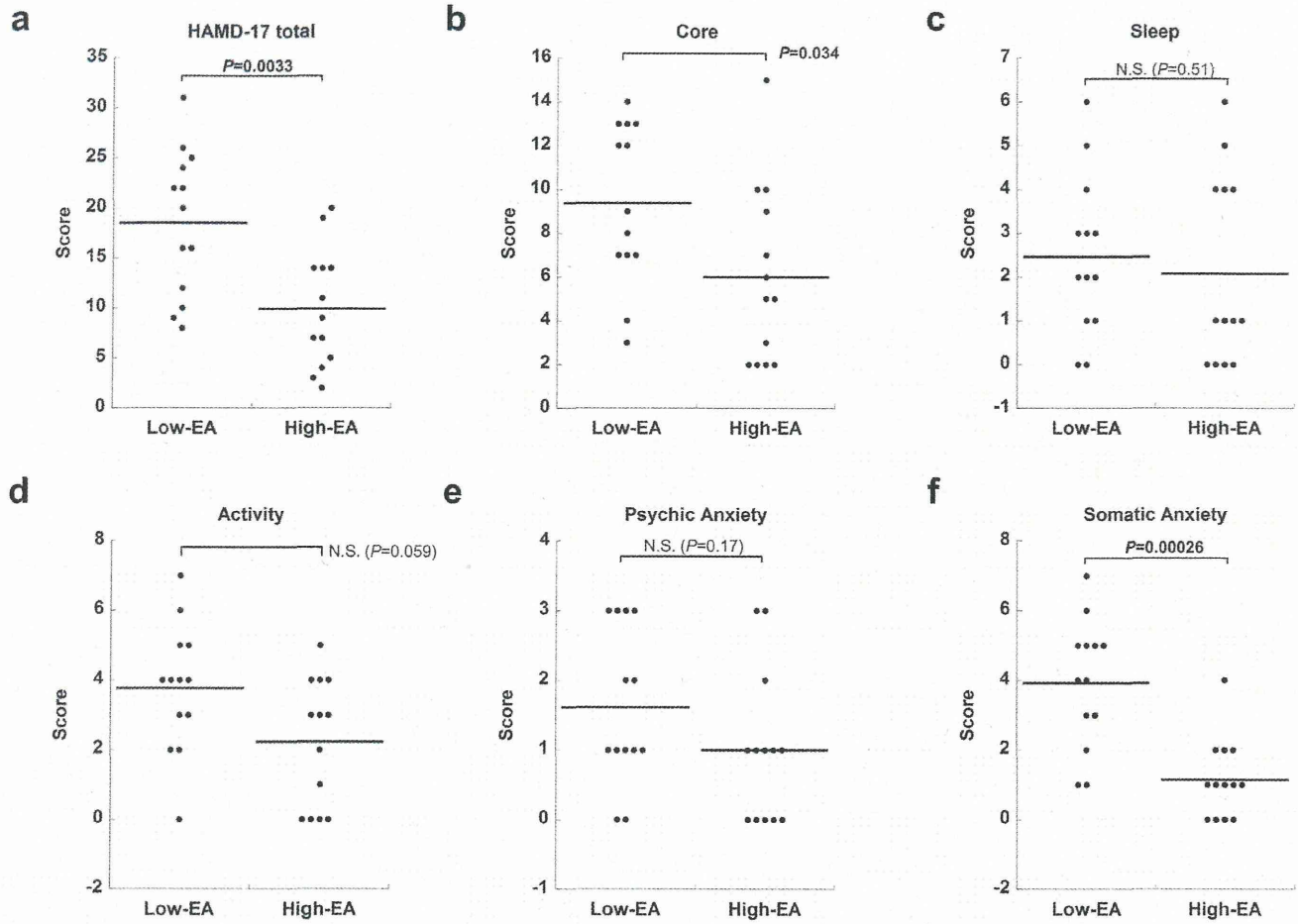

Figure 2 | Dot plots of HAMD-17 total score and subscale scores in High and Low-EA patients. We defined MDD patients with CSF EA values below the 1st quartile as 'Low-EA' ($N = 13$), and MDD patients with CSF EA values above the 3rd quartile as 'High-EA' ($N = 13$) to compare the CSF EA levels with symptoms. Horizontal bars in dot clusters represent mean values of the groups. *P*-values were obtained by the Mann-Whitney *U* test. (a) Low-EA showed a significantly higher total score for HAMD-17 than High-EA ($U = 29.0$, $P = 0.0033$; 95% CI: 3.0 to 15.0). (b) Low-EA showed a significantly higher score for the 'Core' subscale than High-EA ($U = 43.5$, $P = 0.034$; 95% CI: 1.0 to 7.0). There were no significant differences between the two groups for (c) 'Sleep' ($U = 71.5$, $P = 0.51$; 95% CI: −1.0 to 2.0), (d) 'Activity' ($U = 48.0$, $P = 0.059$; 95% CI: 0.0 to 3.0), and (e) 'Psychic Anxiety' ($U = 57.5$, $P = 0.17$; 95% CI: 0.0 to 2.0). (f) Low-EA showed a significantly higher score for 'Somatic Anxiety' than High-EA ($U = 18.5$, $P = 0.00026$; 95% CI: 1.0 to 4.0). Abbreviations: HAMD-17, 17-item Hamilton Depression Rating Scale; CSF, cerebrospinal fluid; EA, ethanolamine; Low-EA, patients with CSF EA values below the 1st quartile; High-EA, patients with CSF EA values above the 3rd quartile; CI, confidence interval for the difference between two medians.

To validate the HPLC measurements, CSF EA levels were measured in a subset of the subjects using CE-TOF-MS. The EA values obtained using CE-TOF-MS and HPLC methods showed a near-perfect correlation ($r = 0.89$, $P < 5 \times 10^{-18}$) in partial correlation analysis, with age and sex as covariates (Supplementary Fig. S3a). Similar to Figure 1a, a significant difference in CSF EA values based on CE-TOF-MS data was observed between the depressed MDD patients and controls ($P = 0.0052$, ANCOVA) (Supplementary Fig. S3b).

Discussion

Several of our findings are potentially of clinical significance. The levels of some CSF amino acids differed between MDD patients and controls. EA (also known as monoethanolamine or 2-aminoethanol), in particular, remained significantly lower in patients than controls after correcting for multiple comparisons ($P = 0.0000011$). Notably, as many as 40% of the depressed patients showed abnormally low levels, and EA levels were significantly lower in depressed patients than remitted patients. When relationships with clinical variables were examined in the patients, the Low-EA group showed higher HAMD-17 and subscale scores compared with the High-EA group. CSF EA did not correlate with the dose of psychotropic drugs, although isoleucine showed a correlation with antidepressants even after correcting for multiple testing. Lastly, CSF EA values were significantly correlated with CSF HVA and 5-HIAA levels in unmedicated subjects.

An early study by Goodnick *et al.*[16] reported that CSF tyrosine levels differed across diagnostic groups (bipolar, unipolar depression, and controls). The authors reported the CSF EA levels; however, there were only two controls in their sample and it is difficult to compare their results with ours. Frye *et al.*[25] reported that CSF glutamate and glycine levels were decreased in patients with mood disorder. By contrast, we found no significant difference in the levels of either amino acid between depressed patients and controls. One of the reasons for the inconsistency may be that the majority of the patients in Frye *et al.*'s study had bipolar disorder. Another reason may be that their subjects were all unmedicated; however, we could not confirm the results of Frye *et al.* even when our unmedicated patients were compared with controls (data not shown). Levine *et al.* reported that depressed patients (MDD and bipolar disorder) showed increased CSF glutamine levels than controls[24]. CSF glutamine levels in our MDD patients were also significantly increased